TEL AVIV UNIVERSITY

The Iby and Aladar Fleischman Faculty of Engineering

The Zandman-Slaner School of Graduate Studies

Solar hydrothermal deconstruction of green macroalgae biomass for biofuel production

A thesis submitted toward the degree

of Master of Science in Environmental Engineering

By

Semion Greiserman

September 2018

TEL AVIV UNIVERSITY

The Iby and Aladar Fleischman Faculty of Engineering
The Zandman-Slaner School of Graduate Studies

Solar hydrothermal deconstruction of green macroalgae biomass for biofuel production

A thesis submitted toward the degree
of Master of Science in Environmental Engineering

By

Semion Greiserman

This research was carried out at the Environmental Engineering program under the supervision of
Prof. Abraham Kribus and Dr. Alexander Golberg

September 2018

Acknowledgments

I would like to thank my supervisors Dr. Alexander Golberg and Prof. Abraham Kribus for the supervision in this research.

I would also like to thank Arthur Rubin and Dr. Meghanath Prabhu for helping me with parts of the analytical methods.

A special thank goes to Michael Epstein who helped me in all aspects of this project. It was a privilege to learn from his knowledge.

This project was supported by the Israeli Ministry of National Infrastructure, Energy and Water Resources.

Abstract

Biomass deconstruction to fermentable sugars is a major challenge for biorefineries. Traditional methods either employ acid or enzymatic hydrolysis, which are expensive and could damage the environment. Thermal hydrolysis is a green technology for biomass deconstruction, carbonization, liquefaction, and gasification. However, subcritical hydrolysis generates a wide range of products from a heterogeneous raw material such as biomass. In this work, Taguchi orthogonal arrays was used for the experimental design and investigation of comparative significance of subcritical water process's temperature, treatment time, solid load and salinity on glucose, xylose, rhamnose, fructose and galactose release from green macroalgae an emerging biorefinery feedstock. We also investigated the impact of the process parameters on the production of 5-hydroxymethylfurfural (5-HMF), an important biofuel intermediate, which, however, is a major fermentation inhibitor. It was found that for all monosaccharides release, the process temperature is the most significant parameter, followed by salinity, solid load and treatment time. Temperature also was the most important parameters for 5-HMF production, followed by residence time, salinity and solid load. The optimum process parameters for maximum release of each monosaccharide and minimum production of 5-HMF was determined. The solid residue (hydrochar) heating value and chemical composition were also determined. Using the results from the experiments a simulation of combined solar electricity generation and fuel (ethanol) production cycle was analyzed. The simulation showed similar electrical efficiency to conventional solar plants with high heat flow contribution for the hydrochar compared to the ethanol.

List of contents

List of symbols

C- Carbon

C_P- Heat capacity ($J \cdot kg^{-1} \cdot K^{-1}$)

H- Enthalpy (J)

H- Hydrogen

$\dot{H}$- Work transfer rate (W)

h- Specific enthalpy ($J \cdot kg^{-1}$)

H_2O- Water

HHV- Higher heating value ($MJ \cdot kg^{-1}$)

HPIC -High pressure ion chromatography

HTC- Hydrothermal carbonization

K_0 – Pre-exponential factor (s^{-1})

K_i – Rate constant (s^{-1})

K_w -Ion product of water ($mol^2 \cdot L^{-2}$)

LHV- Lower heating value ($MJ \cdot kg^{-1}$)

M- Mass (kg)

$\dot{m}$- Mass flow rate ($kg \cdot s^{-1}$)

MPBR- Macroalgae photobioreactor

N- Nitrogen

O- Oxygen

$\dot{Q}$- Heat transfer flow (W)

R - Universal gas constant ($J \cdot K^{-1} \cdot mol^{-1}$)

RPM- Revolutions per minute

S- Sulfur

SN- Signal to noise

T- Temperature (^0C, K)

$\dot{W}$- Work transfer rate (W)

ΔH_R- Enthalpy of reaction ($KJ \cdot mol^{-1}$)

ΔH_{vap}- Enthalpy of vaporization ($KJ \cdot kg^{-1}$)

η- Efficiency

η_I- First law efficiency

η_C- Collector efficiency

η_{el}- Electrical efficiency

List of tables

List of figures

2 Literature review

2.2 Introduction

The world population and energy demand are continuously growing [1].Fulfilling the growing energy demands with minimum environmental impacts requires sustainable energy sources which could replace the traditional polluting ones. Biomass has the potential to fulfil a part of this growing trend and can be used as sustainable source of fuels and chemicals[2]. The main problems with producing energy and fuel from arable biomass is the need of fresh water and the competition on land usage with the food industry [2], [3].

Recent years studies suggest that marine macroalgae (seaweed), which do not compete with food crops for arable land or potable water, can provide a sustainable alternative source of biomass for sustainable fuel [4]. The development of macroalgae feedstocks, enabling processing technologies, and sustainability analysis is still in its infancy, and the development of marine macroalgal biorefinery requires new technological platforms.

A key step in the energy efficient macroalgal biomass conversion to chemicals and biofuels is the deconstruction of cell walls complex carbohydrates [5], [6]. The breaking of long macroalgae polysaccharides is expected to produce fragments with different length, including monosaccharides [7], [8]. These monosaccharides can be used as carbon sources for fermentation of specific molecules at the following steps [9]. However, the released monosaccharides could further degrade to fermentation inhibiting products such as 5-hydroxymethylfurfural (5-HMF), furfural and levulinic acid [10], [11].

Traditional biomass deconstruction relies on thermo-chemical and enzymatic processes [12]–[15]. Those technologies, however, require enzymes [16],which are expensive, or on catalysts such as acids [17], which are non-environmental friendly, cannot be recycled, and needs to be neutralized by bases such as sodium hydroxide [18], [19]. An additional method to deconstruct complex biomass into fermentable chemical intermediates is subcritical thermal hydrolysis [20], [21], in which water at subcritical state is used as a solvent and a catalyst [22].

As thermal hydrolysis does not involve any additional hazardous or expensive chemicals, it can potentially serve as a green process for the macroalgae biomass deconstruction. An

additional hydrothermal process that is widely studied in recent years is the liquification of microalgae which is a unicellular algae with a high lipid content of 20-50% [23], the process is conducted in subcritical water at temperatures of 280-370^{0}C. The process product is biocrude with an energy content close to fossil petroleum, like fossil petroleum the biocrude needs refining for converting to useful biodiesel[24].

The layout of the literature review as can be seen in **Figure 1** will be a discussion of the biomass chosen for this work (green macroalgae) which is being processed using subcritical water. The hydrolysis of the algae and algae carbohydrates to fermentable sugars will be discussed followed by a discussion on the ethanol fermentation process. Hydrothermal carbonization which occurs simultaneously to the hydrolysis process at subcritical conditions will also be discussed. finally, the use of solar energy as a power source for biomass processing will be discussed.

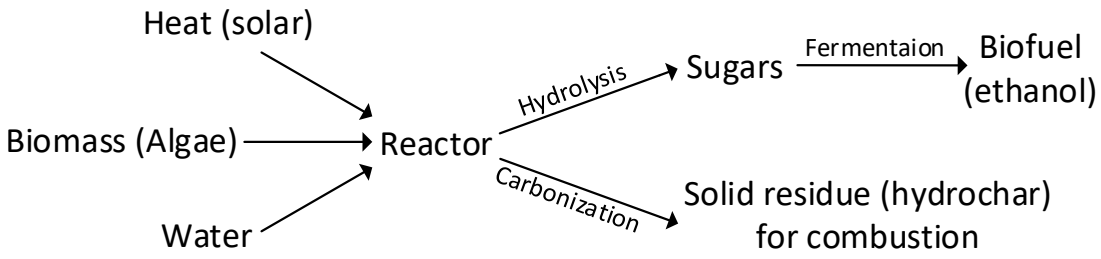

Figure 1- Schematic diagram of the literature review discussion topics

2.3 Green macroalgae chemical composition

Green macroalgae is a marine grown biomass, it can be found all along the Israeli coast line [25]. In this work green macroalgae *Ulva* sp. was used due to its ability to be grown in multiple locations in the world [26] and is considered for multiple biorefinery applications [27] including the fermentation of its hydrolyzed biomass fermentation to ethanol, butanol, and acetone [12], [28]–[30]. The chemical content of the algae can vary depending on the growth conditions such as lighting, water temperature and nutrient flux. The spectrum of green algae biochemical, proximate and ultimate content is summarized in **Table 1**. The higher heating value of green macroalgae ranges between 10.3-16.6 $MJ \cdot kg^{-1}$ [31], [32]. The main carbohydrates in green macroalgae which will be discussed in this work are cellulose, starch and hemicellulose.

Table 1- Biochemical proximate and ultimate analysis of green macroalgae

Analysis	Compound	(wt.%)	Ref.
Biochemical	Carbohydrates	27-54	[32]–[37]
	Lipids	2-10	
	Proteins	11-27	
Proximate	Ash	18-37	
Ultimate	Carbon	26-37	
	Hydrogen	4-6	
	Nitrogen	3-6	
	Oxygen	27-41	
	Sulfur	0.5-5	

A comparison between chemical composition of green macroalgae and the traditional biofuel sources such as corn and sugarcane [2] shows a higher carbohydrates content of 60% and 70% for the corn and for the sugarcane, and lower ash contents with less than 10% for corn and less than 5%, respectively [38], [39], high amount of ash can cause slagging and fouling issues on large scale continues reactors [32]. An advantage is the lack of lignin that is present in corn and sugarcane. Lignin is a highly crossed linked polymer in the cell wall structure that serves as a bonding agent, thus, direct hydrolysis of the cell walls cannot occur and a pretreatment should be applied which complicates the process [40].

2.4 Subcritical water

Subcritical water is water at temperatures of 100-374^{0}C at liquid state [41] (**Figure 2**). To keep water at liquid state pressure is applied. The pressure can be equal to the vapor pressure at a given temperature or higher. At these conditions water can serve as a reaction medium, reactant and catalyst for various chemical reactions and biomass deconstruction processes [22], [42]. As the water temperature increases the physical properties of the water changes, the ion product of water ($K_w[\mathrm{mol}^2 \cdot \mathrm{L}^{-2}]$) which represent the product of H_3O^+ and OH^- (forming by self-ionization) increases by 2-3 orders of magnitude from 10^{-14} at ambient temperature to $10^{-11.5}$ at 150-300^{0}C [43] which leads to the enhancement of reactions involving water as a reactant such as hydrolysis. The viscosity decreases strongly with temperature which leads to better mass transfer and the acceleration of reactions that are limited by mass transfer [44].

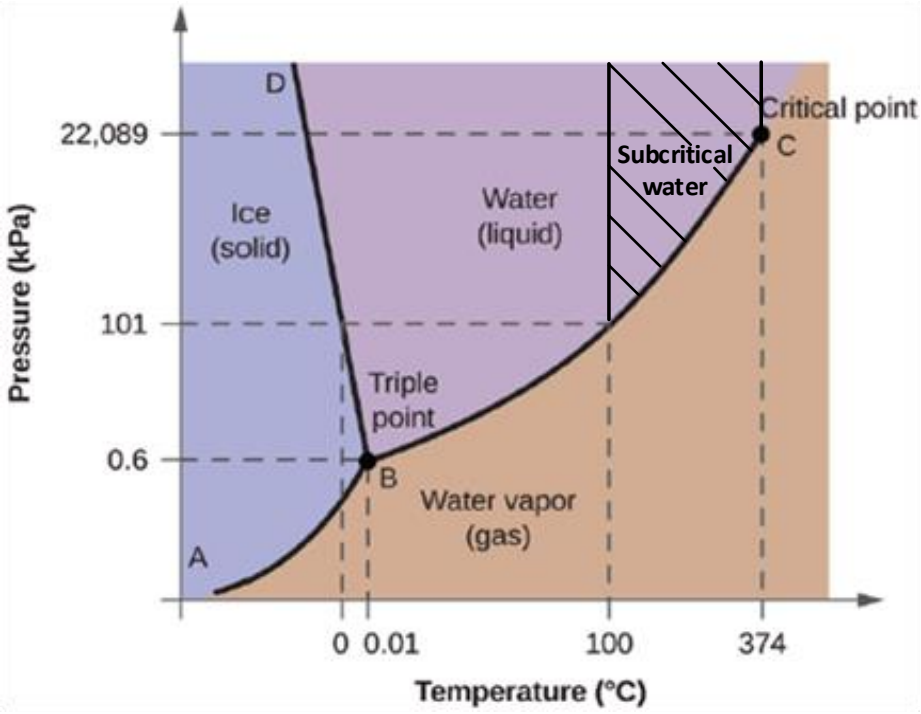

Figure 2- Water phase diagram

2.5 Thermal hydrolysis and degradation

Thermal hydrolysis, which occurs in subcritical water is the break-down of a polymer by reacting with water. The thermal hydrolysis deconstruction of a polymer can be described as a sequence of 2 consecutive first order reactions as showed in **Figure 3**

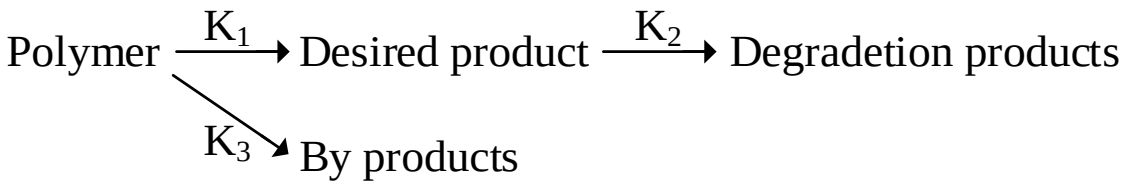

Figure 3- polymer degradation reaction scheme

The most common kinetic model used for polymer degradation is described by Arrhenius equation [45]:

$$K_i = K_{0,i} \cdot exp\left(-\frac{E_{a,i}}{RT}\right) \quad (1)$$

where: K_i is the reaction rate of reaction i, $K_{0,i}$ is the pre-exponential factor of reaction i, $E_{a,i}$ is the reaction activation energy, R is the universal gas constant and T is the temperature. Cellulose (and starch) hydrothermal degradation scheme is shown in **Figure 4** . The cellulose undergoes carbonization and hydrolysis processes which results in hydrochar and glucose, respectively. The glucose can further degrade to hydrochar, isomerate to fructose, dehydrate to HMF or to decompose into acids.

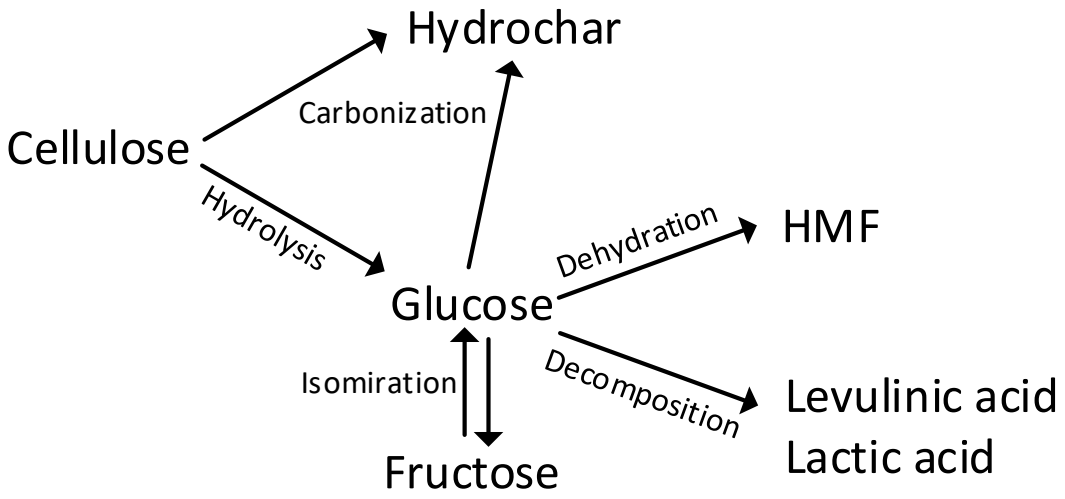

Figure 4- Cellulose hydrothermal degradation scheme

Note: this work was focused on the deconstruction of the algae carbohydrates to monosaccharides which can be than fermented into bio-fuel. Proteins and lipids also undergo hydrolysis and degradation to amino acid, fatty acids and glycerol [46], thus do not affect directly on the monosaccharide release and is not discussed in this study.

2.5.1 Thermal hydrolysis and degradation of Cellulose

As stated above cellulose undergo deconstruction in subcritical water. Hydrolysis of cellulose in subcritical water have been widely studied [47]–[49] .The general hydrolysis reaction can be described by **equation 2**, where cellulose is reacting with water to form a glucose monomer.

$$(C_6H_{10}O_5)_n + nH_2O \rightarrow nC_6H_{12}O_6 \qquad (2)$$

Rogalinski et al [47] made a kinetic study on cellulose degradation to glucose and further degradation products using Arrhenius approach at temperatures of 250-310^{0}C. They found that the activation energies of glucose formation from cellulose and the degradation of glucose to further products are 160.7 kJ·mol^{-1} and 168.7 kJ·mol^{-1}, respectively. The pre-exponential factors obtained were $1.7 \cdot 10^{13}$ s^{-1} and $4.6 \cdot 10^{14}$ s^{-1} for glucose formation and degradation, respectively. The cellulose degradation (water soluble fragments of cellulose including glucose) g activation energy and pre-exponential factor obtained were 163.9 kJ·mol^{-1} and

$7.7 \cdot 10^{13}$ s^{-1}, respectively. Since the activation energies of the cellulose degradation and the glucose formation are similar (163.9 kJ·mol^{-1} and 160.7 kJ·mol^{-1}), it can be concluded that temperature does not have much influence on the selectivity of glucose formation from cellulose. It can be also calculated, for example, that at 250^{0}C and 5 minutes residence time 58% of the degrading cellulose forms glucose, at 220ºC and 60 minutes residence time 62% of the degrading cellulose forms glucose.

Sasaki et al [48] also conducted kinetic study on cellulose decomposition at temperatures of 290-370^{0}C. The activation energy for cellulose degradation obtained was 145.9 ± 4.6 kJ·mol^{-1} and the pre-exponential factor was $10^{11.9\pm0.4}$ s^{-1}.

Gagić et al [49] performed hydrothermal treatment on cellulose at temperatures of 200-300^{0}C with reaction times of 5-60 min. The maximum glucose yield obtained at 250^{0}C with 5 minutes reaction time, was 29% (gram glucose/gram cellulose). The yield of HMF, a degradation product of glucose **(Figure 4)** was 2.7%(w/w). At 200^{0}C and 220^{0}C the maximum glucose yield was obtained at 60 minutes reaction time with 1.9% and 10% (w/w), respectively.

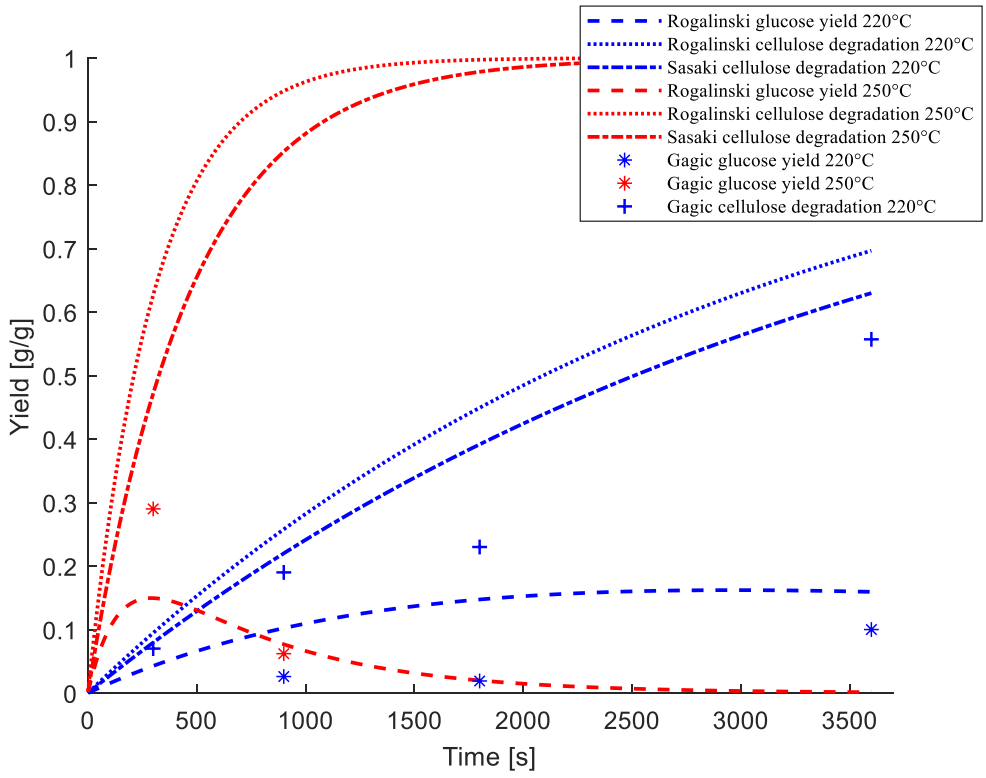

Figure 5- Hydrothermal degradation of cellulose at 220 ºC and 250 ºC

Plotting the results of studies [47]–[49] (**Figure 5**), it can be seen that Rogalinski cellulose degradation kinetics is similar (slightly faster) to this of Sasaki. At 220ºC all 3 studies show similar cellulose degradation results. Comparing the glucose yield with Rogalinski study, Gagić show lower glucose yields at 220ºC. At 250ºC with 5 minutes residence time Gagić showed higher glucose yield and a similar yield was obtained at 15 minutes residence time. Unlike the cellulose degradation results which are consistent, the glucose has an unclear difference which should be further studied. **Table 2** summarizes the kinetic parameters obtained in studies [47], [48].

Table 2- Cellulose and glucose kinetic parameters

Process	Pre-exponential factor K_0 (s^{-1})	Activation energy E_a (kJ· mol^{-1})	Reference
Glucose formation	$1.7 \cdot 10^{13}$	160.7	[47]
Glucose degradation	$4.6 \cdot 10^{14}$	168.7	[47]
Cellulose degradation	$7.7 \cdot 10^{13}$	163.9	[47]
Cellulose degradation	$1 \cdot 10^{11.9 \pm 0.4}$	145.9 ± 4.6	[48]

2.5.2 Thermal hydrolysis and degradation of Starch

Hydrolysis of starch can be also described by **equation 2**. Hydrolyzing starch is easier than cellulose due to the starch weaker structural bonds, thus less energy is required to activate the reaction and the reaction has faster kinetics [47].

Nagamori and Funazukuri [50] hydrolyzed starch at temperatures of 180-240^{0}C with 10 minutes retention time. They found that the glucose production began at 200^{0}C with 0.9% yield (w/w), reached a peak at 220^{0}C with 55% and decreased to 21.1% at 240^{0}C. It was also shown that the yield of HMF increased with temperature from 0.18% at 200^{0}C to 18.6% at 240^{0}C. At constant temperature (220^{0}C) and different residence times it was shown that the yield increased until reaching a maximum at 10 minutes and then decreased. The HMF yield grows with time (at constant temperature).

Rogalinski et al [47] also studied the kinetics of starch hydrolysis at temperatures of 200-270^{0}C. It was found that the activation energies of glucose formation from starch and the degradation of glucose to further products are 134.4 kJ·mol^{-1} and 72.5 kJ·mol^{-1}, respectively. The pre-exponential factors obtained where $1.1 \cdot 10^{11}$ s^{-1} and $1.8 \cdot 10^{5}$ s^{-1} for glucose formation and degradation, respectively. Comparing glucose yields of both studies shows a significant difference with higher yields in Nagamori study as can be seen in **Figure 6.**

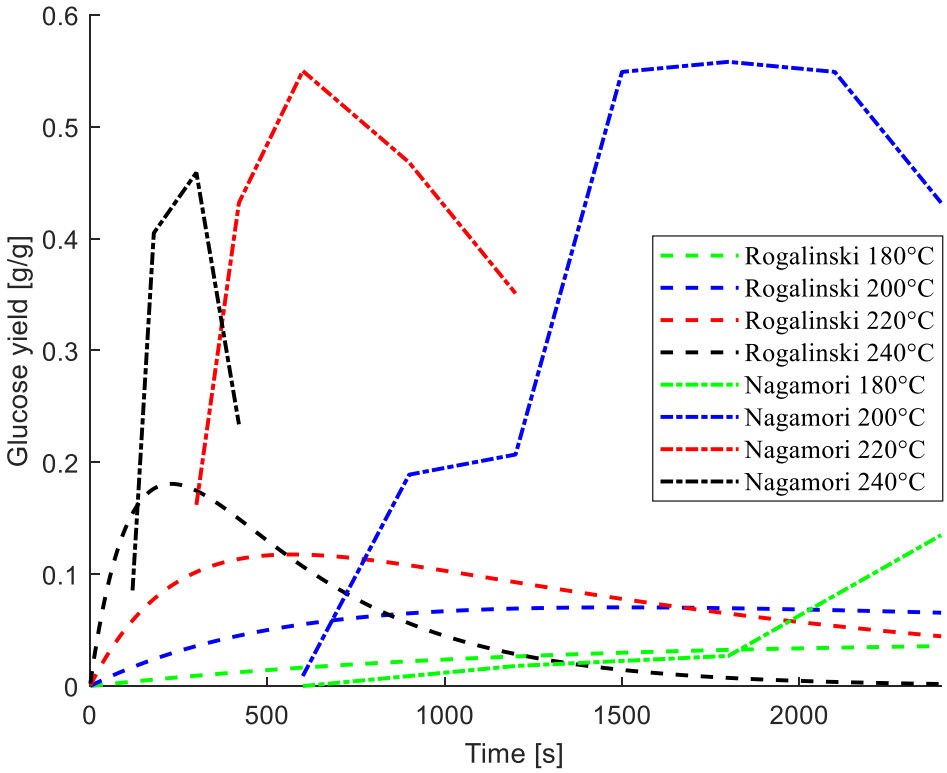

Figure 6- Starch thermal hydrolysis glucose yield

There is a big difference in the glucose yield between the two studies, this can be attributed to the different starch used in the studies. Rogalinski used corn starch while Nagamori used starch from sweet potato.

2.5.3 Thermal hydrolysis and degradation of hemicellulose

Hydrolysis of hemicellulose can be described by **equation 3** where a hemicellulose reacting with water forms xylose (or arabinose) mono-sugar.

$$(C_5H_8O_4)_n + nH_2O \rightarrow nC_5H_{10}O_5 \quad (3)$$

The kinetics and degradations of pure hemicellulose as a polymer in subcritical water wasn't thoroughly studied. Most thermal hydrolysis kinetic studies have been made on thermal acidic hydrolysis [51], [52].

2.5.4 Thermal hydrolysis and degradation of macroalgae

Only few studies have been made on subcritical water hydrolysis of macroalgae. **Table 3** summarizes treatment conditions and sugar yields of the studies.

Table 3- Thermal hydrolysis studies on macroalgae

Algae Specie	**Parameters**	**Results**	**Ref.**
Ulva pertusa (green)	100-200^{0}C 2-12 minutes residence time solid load of 9% (algae weight/total mixture weight)	Maximum glucose yield of 8.5% (glucose weight/algae weight) at 180^{0}C, 10.48 bar and 8 minutes reaction time.	[33]
Saccharina japonica (brown)	180–260°C solid load of 4% (w/w)	Glucose recovery was highest at 180 °C where 1.11% (w/w) was recovered and lowest at 260°C with 0.55% (w/w) recovery.	[8]
Codium fragile (green)	100-240^{0}C 10 minutes residence time	Soluble sugar production began at 170℃ and grew with temperature until a maximum was reached at 210^{0}C where more than 50%(w/w) was converted into soluble sugars. Further increase in temperature decreased soluble sugar yield with 7%(w/w) obtained at 240^{0}C.	[31]

It can be seen from Table 3 that the maximum glucose yield obtained is 8.5%.It can be seen that there is a big difference between ref. [33] and [8] with 8 times more glucose yield at similar

conditions this can be attributed to the high starch concentration in [33] ([8] doesn't specify the amount of starch in the algae) and different algae types (green and brown) which can lead to different hydrolysis kinetics similar to the difference in the kinetics of sweet potato and corn starches as mentioned before. A study by Jiang et al [18] on acidic hydrolysis show similar yield with maximum glucose yield of 9.3% which obtained at 121^0C and 30 minutes residence time. Trivedi et al [53] showed 21.5% reduced sugar yield using enzymatic hydrolysis at temperature of 45^0C and 36 hours residence time.

2.6 Ethanol fermentation

Fermentation is one of the oldest process known to civilization for producing food and beverages and can be dated before 6000 BC in the region between the Black and Caspian seas [54], [55]. Following the conversion of the carbohydrates into monosaccharides it is possible to convert them into various of products including ethanol via fermentation process [56]. Ethanol fermentation was used in this work due to the fact that ethanol fermentation is the most common industrial fermentation process and ethanol is the most widely used biofuel in the world [57]. The process can be described by **equations 4-5** where yeast converts monosaccharides into ethanol and carbon dioxide molecules.

$$C_6H_{12}O_6 \rightarrow 2C_2H_5OH + 2CO_2 \quad (4)$$

$$3C_5H_{10}O_5 \rightarrow 5C_2H_5OH + 5CO_2 \quad (5)$$

Simple mass balance of the reactions shows that the maximum conversion yield of monosaccharides to ethanol is 51.1%(w/w).

Trivedi et al [58] fermented sugars derived from green macroalgae (by enzymatic hydrolysis).They showed a sugar to ethanol conversion of 47.8% with an algae to ethanol conversion of 5.3% (w/w). After fermentation, a distillation process can separate the ethanol from the mixture [59]. Modified car engines can then combust the ethanol directly or as a blend of ethanol and regular gasoline [60].

As stated before, HMF can inhibit fermentation at high concentration. It was found that a concentration of 1-15 g/L inhibits growth and ethanol fermentation of different strains of Saccharomyces cerevisiae (yeast) [61], [62].

2.7 Hydrothermal carbonization

Hydrothermal carbonization (HTC), which was first described by Friedrich Bergius in 1913 [63] is a process occurring in subcritical water heated to temperatures of 180-260^{0}C. In this process the carbon fraction in the solid residue (hydrochar) is enhanced due to the release of water molecules from carbohydrates or monosaccharides , and thus providing carbon-rich products [64] and leading to an increase in the residue's calorific value. Several stoichiometric equations can describe the carbonization process. **Equation 6** was suggested by Bergius:

$$(C_6H_{12}O_5)_4 \rightarrow C_{21}H_{16}O_2 + 3CO_2 + 12H_2O\ ;\ \Delta H_R = -297.9\frac{kJ}{mol} \quad (6)$$

Two more equations where proposed by Ramke et al [65] (**equation 7**) and Titirici et al [66] (**equation 8**).

$$C_6H_{12}O_6 \rightarrow C_6H_2O + 5H_2O\ ;\ \Delta H_R = -1040\frac{kJ}{mol} \quad (7)$$

$$C_6H_{12}O_6 \rightarrow C_6H_4O_2 + 4H_2O\ ;\ \Delta H_R = -950\frac{kJ}{mol} \quad (8)$$

HTC is an exothermic process which makes it a self-sustained reaction. To activate the reaction, a temperature of 180^{0}C is needed to overcome the activation energy. Many studies have been made in converting biomass [67] and biomass waste [68] into hydrochar and in recent years studies have been made on carbonization of macroalgae. **Table 4** summarizes HTC studies on macroalgae in recent years.

Table 4- HTC studies on macroalgae

Algae Specie	Parameters	Results	Reference
Codium fragile (green)	100-240^{0}C 10 minutes residence time	HHV of the residue increased constantly between 140-230^{0}C, till a maximum of 22.6 MJ kg^{-1}, an increase of 6 MJ kg^{-1} compared to the HHV of untreated biomass.	[31]
Laminaria digitate *Laminaria hyperborean* *Alaria esculenta* (brown)	200^{0}C ,250^{0}C 60 minutes residence time solid loads of 10%(w/w)	The hydrochar yield (w/w) was 22-39% at 200^{0}C and 18-32% at 250^{0}C. The char HHV increased from 11-14 MJ kg^{-1} to 21-23 MJ kg^{-1} at 200^{0}C and to 22.6-26.5 MJ kg^{-1} at 250^{0}C.	[69]
Sargassum horneri (brown)	180-210^{0}C 2-16 hours residence time solid loads of 4.7-16.6% (w/w) different concentration and grain sizes of citric acid	HHV increased from 17.4 MJ kg^{-1} to 20.8-25.1 MJ kg^{-1}. The hydrochar yield(w/w) obtained was 32.7-52.3%	[70]

It can be concluded that with increasing temperature the HHV increases and the hydrochar yield decreases. At 200^{0}C the HHV gain is 6-10.7 MJ kg^{-1} compared to the initial biomass. Comparing the total heat that can be produced by combusting a biomass unit with the hydrochar that was produced from this biomass unit a total of 33-60% of the combustion heat is lost. Although the total combustion heat is lost the hydrochar energy density is increased, which makes it more suitable for co-combustion with coal than untreated biomass [71].

2.8 Solar energy for biomass processing

In order to obtain the conditions for algae deconstruction process a heat source is needed. Solar energy can be used as a renewable heat source for various processes including chemical reactions [72]. The solar radiation can be applied directly or indirectly for the process. To obtain high temperatures in a chemical reactor (directly or indirectly) a concentration of the solar radiation is needed. Today the main concentration methods for solar thermal power plants are parabolic trough and solar tower. In the parabolic trough technology solar radiation is concentrated by 70-80 times, the heat transfer fluid is usually a synthetic oil with operational temperatures of 290-390^{0}C. Heat storage, if needed, can be done indirectly using molten salt.

In solar tower technology radiation can be concentrated by >1000 times. In this case the heat transfer fluid is usually water (which can be directly heated, and the resulted steam enters a turbine) or molten salt at temperature of 290-560^{0}C, here the heat storage can be done directly with the heated salt [73], [74].Studies of solar driven gasification of biomass have been conducted at high temperatures of 800-1177^{0}C, at this condition the biomass is converted mainly to hydrogen, carbon monoxide, carbon dioxide and methane gases with conversions rates of up to 95% [75]–[77].

Table 5- Common solar power plant technologies summary

Technology	Heat transfer fluid	Operational temperatures (^{0}C)	radiation concentration	References
Parabolic trough	Thermal oil	290-390	70-80	[73], [74]
Solar tower	Molten salt, Water	290-560	>1000	

Giaconia et al [78] conducted a conceptual study on coupling solar energy for liquefaction of micro-algae at temperature of 350^{0}C using concentrated solar power technology with molten salt as heat transfer fluid (hot storage at 410^{0}C and cold storage at 340^{0}C. The product of the liquefaction process is biocrude with higher heating values of 30-36 MJ kg^{-1}. They showed a full plant design and analysis including economic study with different solar field areas and different heat storage times. The plant processes 2.14 kg/s mixture of water and microalgae (85% water,15% algae) micro-algae with a constant power of 800kW supplied for the liquification by the solar field. The biocrude yield is 37.5% (biocrude wt./microalgae wt.).

It was found that the minimum selling price for the produced biocrude is 2.19 US$/kg (The plant efficiency was not calculated). Also, it was demonstrated that concentrated solar power plant using molten salt mixture can serve as a heat source for chemical processing (within the salt stability temperature intervals).

2.9 Literature gaps and objectives

Studies on deconstruction of carbohydrates and macroalgae focus mainly on the effect of temperature and residence time on the product yield. Moreover, no detailed monosaccharide products were analyzed for thermal hydrolysis of algae. At the present work the effect of the solid load and water salinity (i.e. using sea water and not pure water as reaction medium) were also be examined (together with temperature and residence time) with the attempt to find the best conditions for all algae monosaccharide release and the examination of each parameter affect individually using Taguchi orthogonal arrays method, This will give a better understanding on the algae hydrolysis process and what are the important parameters for a desired output.

Also, a main gap is an integration of macroalgae thermal processing with a heat source to see the efficiency of such process and the plausibility of using renewable heat sources such as solar energy for bio-fuel production from macroalgae, in this work a demonstration of a simplified solar powered macroalgae deconstruction cycle for bio-fuel production will be examined.

3 Experimental

3.2 Macroalgae biomass

Green macroalgae *Ulva* sp.,collected from a shore in Haifa, Israel, identified morphologically in ref [25], was grown under controlled conditions using macroalgae photobioreactors (MPBR) (length 100 cm, thickness 200 mm, width 40 cm) incorporated in a building's south wall under daylight conditions .The detailed description of the cultivation system appears in ref [79]. Nutrients were supplied by adding ammonium nitrate (NH_4NO_3) and phosphoric acid (H_3PO_4), to maintain 6.4 g m^{-3} of total nitrogen and 0.97 g m^{-3} of total phosphorus in the seawater. The sole CO_2 source was bubbled air. Other conditions such as pH (8.2), salinity, and air flow rate (2-4 L/min) were maintained steady in all the reactors. All biomass was dried at 40ºC to constant weight.

3.3 Experimental system description

Subcritical water batch experimental system was used for biomass treatment (**Figure 7, Figure 8**). The experimental system consists of a 0.25 liter "Zhengzhou Keda Machinery and Instrument Equipment CJF-0.25" batch reactor heated by an electric heater (Keda Machinery, China). The temperature is controlled and measured with an MRC TM-5005 digital temperature gauge using "Watlow" 1/16" thermocouple type K. The pressure is constantly measured using "MRC PS-9302" pressure gauge with "MRC PS100-50BAR" sensor. A magnetic coupling drive was used to mix the slurry inside the pressure reactor (In all experiments the stirrer was set at 70 RPM). The magnet coupling is cooled using a chiller (Guangzhou Teyu Electromechanical Co., Ltd Cw-5200ai, China). The reactor has 2 gas sampling ports and 1 liquid sampling line. The liquid line goes through a condenser (also cooled by the chiller) and a cold trap, before entering the sampling tube. The gas is collected with a 1-liter sampling bag. The gas line goes through a condenser and a cold trap before reaching the gas sampling bag. An MRC ST-85 vacuum pump (0.13 mbar) is used to drain air in the system before each experiment. In each experiment a mixture of dry algae and water was inserted into the reactor. The reactor was filled with 100 grams of algae and water mixture, then heated to the selected temperature and after a desired residence time the sample was taken for analysis.

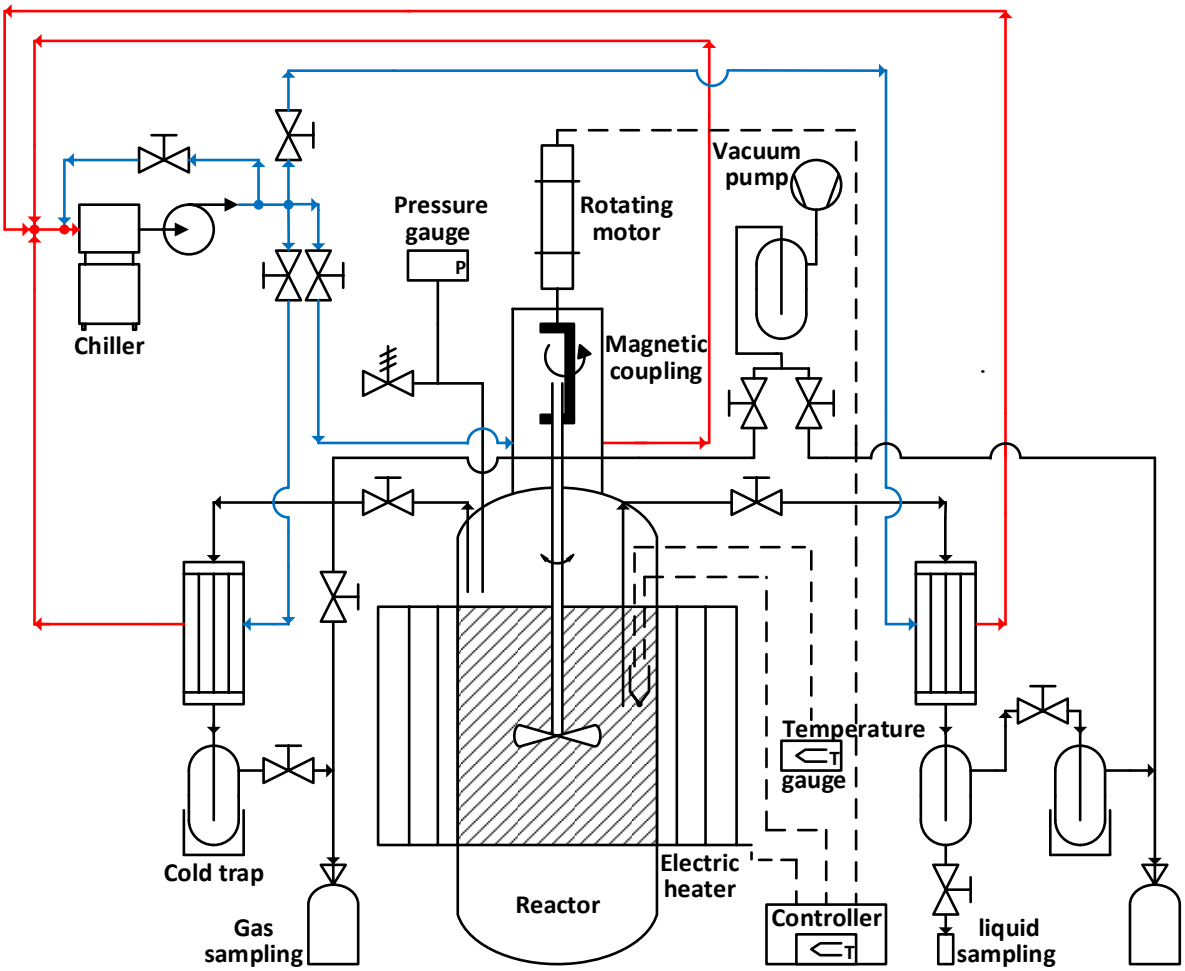

Figure 7-Experimental system schematic diagram

1.Electric heater 2. Reactor 3. Stirrer motor 4. Heat exchanger 5. Pressure sensor 6. Thermocouple 7. Temperature gauge 8. Pressure gauge 9. Controller

Figure 8- Experimental system

3.4 Taguchi method experiments

The goal in these series of experiments was to determine the effects of subcritical water hydrolysis process parameters: temperature, treatment time, salinity and solid load on the release of monosaccharaides from the *Ulva* sp. biomass (green algae). The possible range of process parameters and their combinations is large. Therefore, to decrease the number of experiments, but still be able to evaluate the impact of each parameter independently, Taguchi Robust Design method for the experimental design [80] was applied. A key feature of the Taguchi method is the design of the experiment where process factors are tested with orthogonal arrays. This design allows for the follow up analysis that prioritizes the comparative impact of the process parameters on the yields. The tested parameters and their levels are shown in **Table 6. Table 7** shows the experimental layout.

Table 6- Taguchi tested parameters

level / Parameter	1	2	3
Temperature (^{0}C)	170	187	205
Residence time(min)	20	40	60
Solid load (%algae weight/total mixture weight)	2	5	8
Salinity (% sea water)	0	50	100

Table 7- Taguchi experimental setup

Experiment #	Temperature (^{0}C)	Solid load (% algae weight/total mixture weight)	Residence time(min)	Salinity (% sea water)
1,10	170	2	20	0
2,11	170	5	40	50
3,12	170	8	60	100
4,13	187	2	40	100
5,14	187	5	60	0
6,15	187	8	20	50
7,16	205	2	60	50
8,17	205	5	20	100
9,18	205	8	40	0

In Taguchi design of experiment algorithm, the best parameter setting is determined using signal-to-noise ratio (SN), it was defined as a mean to measure variation of the outcome based on the assumption that there is no ideal relationship between the input signal and the outcome. The SN ratio was derived from the quadratic loss function and represents the deviation product between a function of the signal and the variance of the error caused by the noise factors. In other words, the SN ratio represents the impact of a controlled parameters (signal) (in our case: temperature, treatment time, salinity and solid load) on the desired outcome with the minimalization of the outcome variation due to any uncontrollable factors (noise), these factors can include in our case variations in the algae grain size and the reactor heating rate. In our experiments, in order to maximaize the outcome we used Taguchi algorithm of "the larger the better" type. The ratio SN is determined independently for each of the process outcomes (OUT_max) to be optimized. These process outcomes are concentrations of glucose, rhamnose, galactose, xylose, fructose, HMF and total sugars. In the current context, maximizing SN corresponds to obtaining the maximum concentration and extraction yields of monosaccharides. The ratio SN of a specific process outcome OUT in experiment j was calculated by:

$$SN^{OUT\_max}(j) = -10 \cdot \log\left[\frac{1}{\#Reps}\sum_{Rep=1}^{\#Reps}\frac{1}{(m_{Rep})^2}\right] \qquad 1 \le j \le K \qquad (9)$$

Where K is the number of experiments (in our case K=9; #Reps is the number of experiment repetitions (in our case #Reps=2) and m_{Rep} is the measurement of the process outcome (OUT) in the specific repetition Rep of experiment j.

When the process condition is optimized for reducing the concentration of produced toxic substances (OUT_max), for example, hydro methyl furfural (HMF) in our example, "the smaller the better" type algorithm is used. In this case, the ratio SN of a specific process outcome OUT in experiment j was calculated by:

$$SN^{OUT\_min}(j) = -10 \cdot \log\left[\frac{1}{\#Reps}\sum_{Rep=1}^{\#Reps}(m_{Rep})^2\right] \qquad 1 \le j \le K \qquad (10)$$

Considering a process parameter P (temperature, treatment time, salinity and solid load as appears in Table 1 and assuming that P has a value of L in n (P, L) experiments (i.e. temperature=170 appears in 3 experiments: P=temperature L=170 and n=3). Let J (P, L) be the set of experiments in which process parameter P was applied at level L. Let:

$$SN^{OUT}(P,L) = \frac{1}{n(P,L)}\sum_{j \in J(P,L)} SN^{OUT}(j) \qquad (11)$$

be the average ratio SN for concrete level L of parameter P. The sensitivity (Δ) of each outcome (OUT) with respect to the change in a parameter P is calculated as:

$$\Delta^{OUT}(P) = Max\{SN^{OUT}(P,L)\} - Min\{SN^{OUT}(P,L)\} \qquad (12)$$

Ranking (on the scale of 1-4, where 1 is the highest) was assigned to the process parameters according to the ranges obtained.

3.5 Analytical

3.5.1 Monosaccharides analysis

For monosaccharides and hydroxymethyl furfural (HMF) analysis, hydrolysates were thawed, and an aliquot was diluted 20/50 times in ultrapure water before being filtered through a 0.22µm syringe-filter in HPIC vials. Monosaccharides and HMF content in the hydrolysates were monitored by HPAEC-PAD (High-Pressure Anion-Exchange Chromatography coupled with Pulsed Amperometric Detection) using a Dionex ICS-5000 platform with an analytical column and its corresponding guard column. Calibration curves were produced for each sugar with internal standards. The quantified sugars were rhamnose, arabinose, galactose, glucose, xylose, fructose and HMF.

3.5.2 Hydrochar and water-soluble solid mass recovery

At the end of each experiment a liquid sample was taken and dried for calculation of the water-soluble solids. The residue (solid and liquid) was dried at 40^0C. The hydrochar yield was then calculated by subtracting the water-soluble solids (which were calculated by multiplying the amount of solid left from the dried liquid sample by the quotient of the total liquid dried in the residue and the liquid sample taken) from the total solid left after drying.

3.5.3 Elemental analysis

Elemental analysis (CHNS) was done at the Technion, Chemical, and Surface Analysis Laboratory using Thermo Scientific CHNS Analyzer (Flash2000)**.** The oxygen content can be determined by difference.

$$\%O=100\%-(\%C+\%H+\%N+\%S+\%Ash) \quad (13)$$

3.5.4 Higher heating value ash and moisture content

For caloric value, ash and moisture analysis, untreated algae and hydrochar (separated from the water-soluble solids by water washing) were dried at 40ºC to constant weight and analyzed for energy content (HHV) using Parr 6200 Isoperibol Calorimeter according to ASTM D5865 – 13 standard. Ash and moisture content were analyzed according to D5142 standard. The analysis was conducted by a certified laboratory of Israel Electric Company.

For validation of the values obtained by the Israeli Electric company, the HHV was also calculated using the following correlations [81]:

Boie:

$$Q = 151.2C + 499.77H + 45S - 47.7O + 27N \quad (14)$$

Grummel and Davis:

$$Q = \left[\frac{654.3H}{(100 - A)} + 424.62\right] \cdot \left[\frac{C}{3} + H - \frac{O}{8} + \frac{S}{8}\right] \quad (15)$$

Where:

Q is the gross heating value [Btu/lb]

C, H, N, S, O, A are the weight percentage of carbon, hydrogen, nitrogen, sulfur, oxygen and ash respectably.

3.5.5 Starch analysis

The algae were grounded to fine powder using a mortar and pestle with the help of liquid nitrogen and starch content was determined using a total starch assay kit (K-TSTA-100A, Megazyme, Ireland) according to AACC Method 76-13.01.

4 Result and discussion

4.2 Experiment measured conditions

Table 8 shows the actual measured parameters in the experiments. The sampling temperature correlates to the theoretical vapor pressure of water meaning no major gas formation occurred during the experiment. The reactor temperature profile in the experiments can be seen in **Figure 9.** The temperature rises linearly until reaching the desired temperature where it stabilized. The rector heats up slowly with 40 minutes heating time until reaching a temperature of 150^0C.

Table 8- Taguchi experiments measured conditions

Block	Exp #	Temperature* [^{0}C]	Solid load (% dry algae weight/total mixture weight)	Pressure (bar)	Residence time** (min)	Salinity % of sea water (100%= 38 gr/L sea salts)
1	1	163	2	6.6	20	0
	2	170	5	7.7	40	50
	3	172	8	8.1	60	100
	4	187	2	11.4	40	100
	5	189	5	12.3	60	0
	6	180	8	10	20	50
	7	204	2	16.4	60	50
	8	194	5	13.7	20	100
	9	208	8	18.2	40	0
2	10	166	2	7.1	20	0
	11	171	5	8.2	40	50
	12	173	8	8.2	60	100
	13	187	2	11.7	40	100
	14	192	5	13.1	60	0
	15	184	8	11.1	20	50
	16	206	2	17.7	60	50
	17	197	5	15.3	20	100
	18	209	8	20.4	40	0

* Sampling measured temperature.

** Measured from the time reaching the desired temperature.

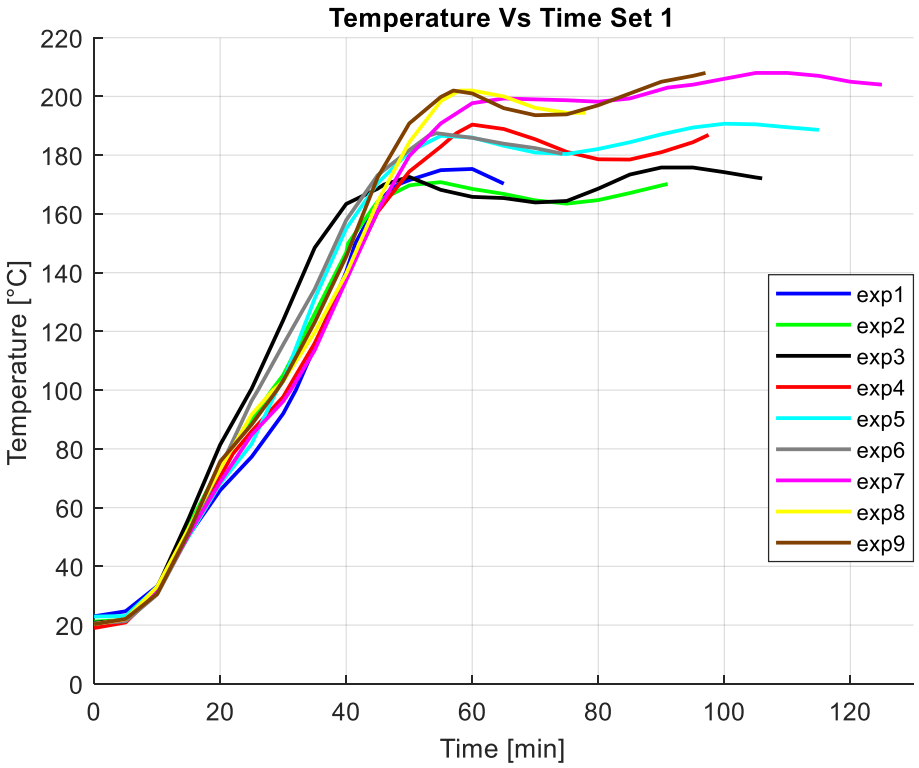

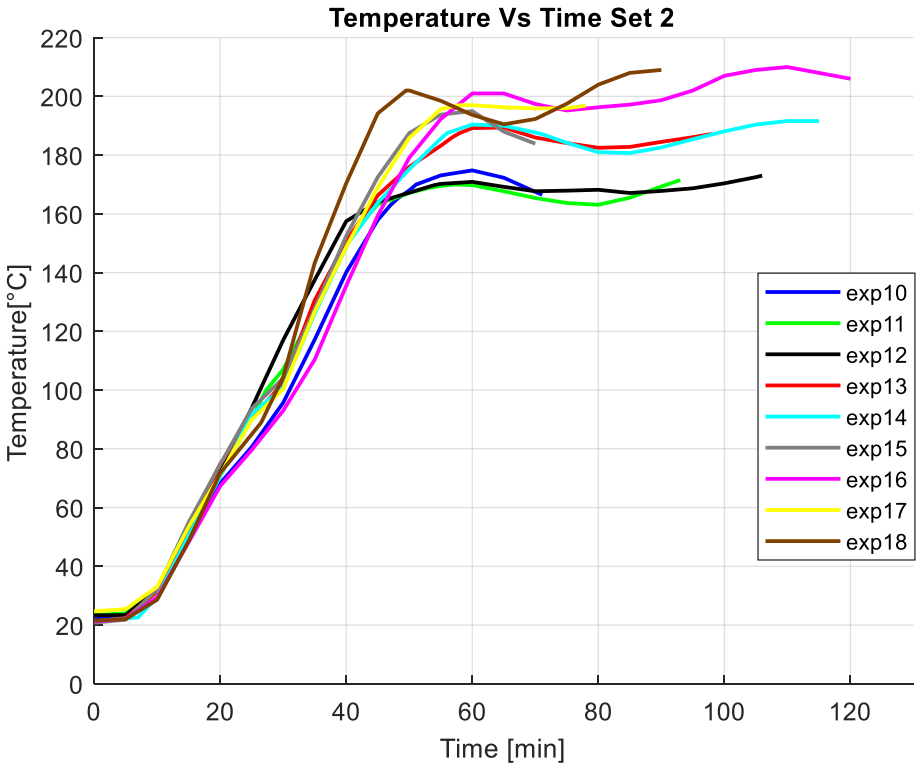

Figure 9- Reactor temperature profile in Taguchi experiments

4.3 Monosaccharide release

The monosaccharides and HMF products are showed in **Table 9**.

Table 9- Measured products from Ulva hydrolysis

Exp #	Glucose mg/g	Rhamnose mg/g	Galactose mg/g	Xylose mg/g	Fructose mg/g	Total yield	HMF
1	2.02	1.13	0	1	1.69	5.84	0
2	1.37	0.93	0.02	0.94	0.74	4.00	0.16
3	6.11	0.9	0.5	1.36	1.27	10.14	1.3
4	4.19	1.7	0.41	0.6	1.15	8.05	2.3
5	2.43	0.09	0.1	0	0.95	3.57	2.58
6	1.45	0.97	0.5	0.65	0.42	3.99	0.72
7	0	0	0	0	0	0.00	3.5
8	2.12	0	0.01	0	0.82	2.95	4.22
9	0.21	0	0	0	0	0.21	2
10	2.76	0.98	0	1	2.35	7.09	0
11	1.22	1.35	0.1	0.93	0.81	4.41	0.58
12	2.67	3	0.46	1.6	0.78	8.51	1.31
13	5.64	2	0.33	0.62	1.93	10.52	5
14	2.22	0.32	0.04	0	0.88	3.46	3
15	5.77	1.8	0.48	0.57	1.62	10.24	3.77
16	0	0	0	0	0	0.00	0
17	2.57	0	0	0.22	1.1	3.89	9.45
18	0.1	0	0	0	0.03	0.13	3.2

In almost all experiments glucose was the major monosaccharide released with maximum sugar yield of 6.11 mg/g obtained in experiment number 3, followed by rhamnose, fructose and xylose with maximum yield of 3, 2.35 and 1.6 mg/g, respectively. Galactose had the lowest yield in most experiments with maximum yield of 0.5 mg/g. The maximum total monosaccharide yield obtained in experiment number 13 with 10.52 mg/g and the maximum HMF yield was 9.45 mg/g obtained in experiment number 17. The average monosaccharide

yields of the repeated experiments can be seen in **Table 10**. **Figure 10** shows the hydrolysate of the experiments with darker liquid color obtained at higher solid loads.

Table 10- Taguchi hydrolysis average products yield

Exp #	Rhamnose mg/g	Galacatose mg/g	Glucose mg/g	Xylose mg/g	Fructose mg/g	Total Sugars mg/g	HMF mg/g
1,10	1.05	0	2.39	1	2	6.47	0
2,11	1.14	0.06	1.29	0.94	0.77	4.22	0.37
3,12	1.95	0.48	4.39	1.48	1	9.34	1.3
4,13	1.86	0.37	4.92	0.51	1.54	9.31	3.68
5,14	0.2	0.07	2.32	0	0.91	3.52	2.81
6,15	1.39	0.49	3.61	0.61	1.02	7.12	2.25
7,16	0	0	0	0	0	0	1.75
8,17	0	0	2.34	0.11	0.96	3.43	6.83
9,18	0	0	0.16	0	0.01	0.17	2.6

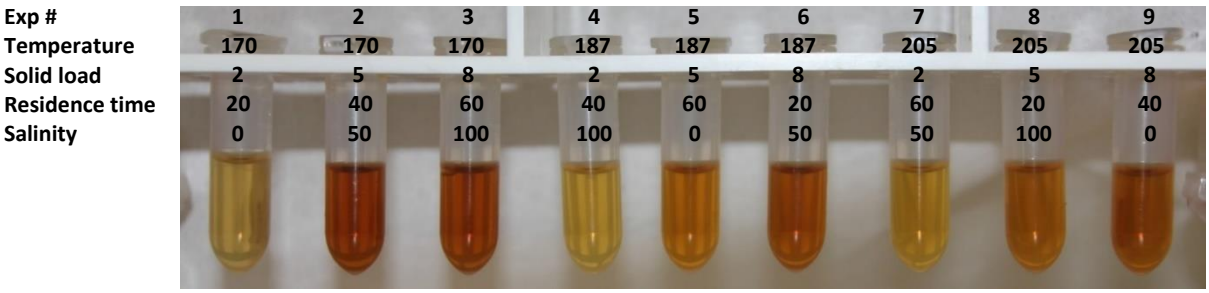

Temperature in ºC, solid load in % dry algae weight/total mixture weight, residence time in minutes and salinity in % of sea water.

Figure 10- Hydrolysis samples

4.4 Taguchi analysis

As stated before green macroalgae *Ulva* sp. biomass major polymer composition includes cellulose (with glucose monomers), hemicellulose (xylose, galactose, rhamnose and sometimes other monosaccharides as monomers), starch (with glucose monomers), and proteins (with amino acids as monomers) [82], [83]. Therefore, hydrolysis of whole *Ulva* sp. biomass is expected to release these monomers to the solution. Further dehydration of hexoses and pentoses leads to the formation of HMF and furfurals, respectively [84]. The impact of process parameters: temperature, residence time, solid load and salinity on the monosaccharide and HMF production was determined.

Glucose was the major released monosaccharide from *Ulva* sp. biomass under the tested conditions. The maximum average yield achieved was 4.92 ± 0.73 mg glucose/g dry algae, when 187^{o}C, 2% solid load, 40 min residence time and 100% salinity were used. Taguchi analysis (**Table A1 in Appendix 1**) showed that treatment temperature was the most important factor for maximum glucose yield, followed by salinity, then solid load and residence time. The optimum parameters for the maximum glucose release are shown in **Table A8.**
Comparing the result to an *Ulva* thermal hydrolysis study [33] shows a big difference with 8.5% glucose yield obtained at 180 ^{o}C, 8 minutes residence time and 9% solid load. The big difference can be partly contributed to higher starch concentration in [33] with 4.5 times more starch than in this study. More similar result obtained compared to study [8] with 1.11% glucose yield at 180 ^{o}C, however the carbohydrate content was not specified. Also study [8] used different algae which could lead to difference in the results.

The maximum average yield achieved for rhamnose, a rare sugar derived from the deconstruction of ulvan in our process, was 1.95 ± 1.05 mg rhamnose/g dry algae when 170^{o}C, 8% solid load, 40 min residence time and 100% salinity were used. Taguchi analysis (**Table A2**) showed that the temperature was the most important factor for maximum glucose yield, followed by salinity, then solid load and residence time. The optimum parameters for the maximum rhamnose release were determined as 170^{o}C, 2% solid load, 40 min residence time and 100% salinity (**Table A8**).

The maximum average yield achieved for galactose, a sugar derived from the deconstruction of hemicellulose in our process, was 0.49 ± 0.01 mg galactose/g dry algae), when 187^{o}C, 8%

solid load, 20 min residence time and 50% salinity were used. Taguchi analysis (**Table A3**) showed that temperature was the most important factor for maximum glucose yield, followed by salinity, then solid load and residence time. The optimum parameters for the maximum galactose release were determined as 187^{o}C, 8% solid load, 60 min residence time and 100% salinity (**Table A8**).

The maximum average yield achieved for xylose, a sugar derived from the deconstruction of hemicellulose in our process, was 1.48±0.12 mg xylose/g dry algae (**Table 9** exp #3 and #12), when 170^{o}C, 8% solid load, 60 min residence time and 100% salinity were used. Taguchi analysis (**Table A4**) showed that temperature was the most important factor for maximum glucose yield, followed by salinity, then solid load and residence time. The optimum parameters for the maximum xylose release were determined as 170^{o}C, 8% solid load, 20 min residence time and 100% salinity (**Table A8**).

The maximum average yield achieved for fructose, a sugar derived from the deconstruction of cellulose and starch in our process, was 1.54±0.39 mg fructose/g dry algae (**Table 9** exp #4 and #13), when 187^{o}C, 2% solid load, 40 min residence time and 100% salinity were used. Taguchi analysis (**Table A5**) showed that temperature was the most important factor for maximum glucose yield, followed by salinity, then solid load and residence time. The optimum parameters for the maximum fructose release were determined as 170^{o}C, 5% solid load, 40 min residence time and 100% salinity (**Table A8**).

Note: as stated in the gaps, no detailed monosaccharide products were made for thermal hydrolysis of algae. Thus, no comparison for rhamnose, galactose xylose and fructose to literature was made.

The minimum yield of produced HMF, potentially corresponding to the minimum toxicity of the hydrolysate for subsequent fermentation was 0 mg HMF/g dry algae (**Table 9** exp #1 and #10), when 170^{o}C, 2% solid load, 20 min residence time and 0% salinity were used. Taguchi analysis (**Table A7**) showed that temperature was the most important factor for minimum HMF yield, followed by residence time, then salinity and solid load. The optimum parameters for the minimum HMF production were determined as 170^{o}C, 2% solid load, 20 min residence time and 0% salinity (**Table A6**). The maximum concentration of HMF, 6.83±2.61 mgHMF/g dry

algae was detected at experiments 8 and 17, when 205^{o}C, 5% solid load, 20 min residence time and 100% salinity were applied (**Table 9**). This is equivalent to 341.5±130.5 mgHMF/L of hydrolysate, which is lower than reported levels of HMF (1-15 g/L) that inhibit growth and ethanol fermentation of different strains of *Saccharomyces cerevisiae* [61], [62].

The maximum total sugar yield of 9.34±0.81 mg sugars/g dry algae (**Table 9** exp #3 and #12), when 170^{o}C, 8% solid load, 60 min residence time and 100% salinity were used. At these conditions 1.3 ±0.1 mg HMF/g dry algae were detected (**Table 9**). Taguchi analysis (**Table A7**) showed that temperature was the most important factor for maximum total sugars yield, followed by salinity, then solid load and residence time. The optimum parameters for the maximum total sugars release were determined as 170^{o}C, 5% solid load, 40 min residence time and 100% salinity (**Table A8**).

The results also show that increasing the temperature and residence time above certain values (specific for each sugar) led to the decrease of sugars concentrations. However, increase in temperature and time led to the increase of HMF formation. These results are consistent with previous report on the HMF formation from partial hexose degradation [85] which shows increase in HMF yield with time.

The study shows that subcritical water treatment of green macroalgae *Ulva* sp. biomass leads to the partial deconstruction of heterogeneous macroalgae to simple, fermentable monosaccharides. In addition, 5-HMF is produced as a part of degradation reactions. The optimum parameters for the maximum total sugars release were determined as 170^{0}C (810 kPa abs.), 5% solid load, 40 min residence time and 100% salinity. Taguchi analysis showed that temperature was the most important factor for maximum total sugars yield, followed by salinity, then solid load and residence time. Higher reaction temperatures and long residence times lead to sugars degradation and formation of 5-HMF.

Note: experiment with different type of green algae (*Cladophora*) and with a different experiment design can be seen in appendix 4

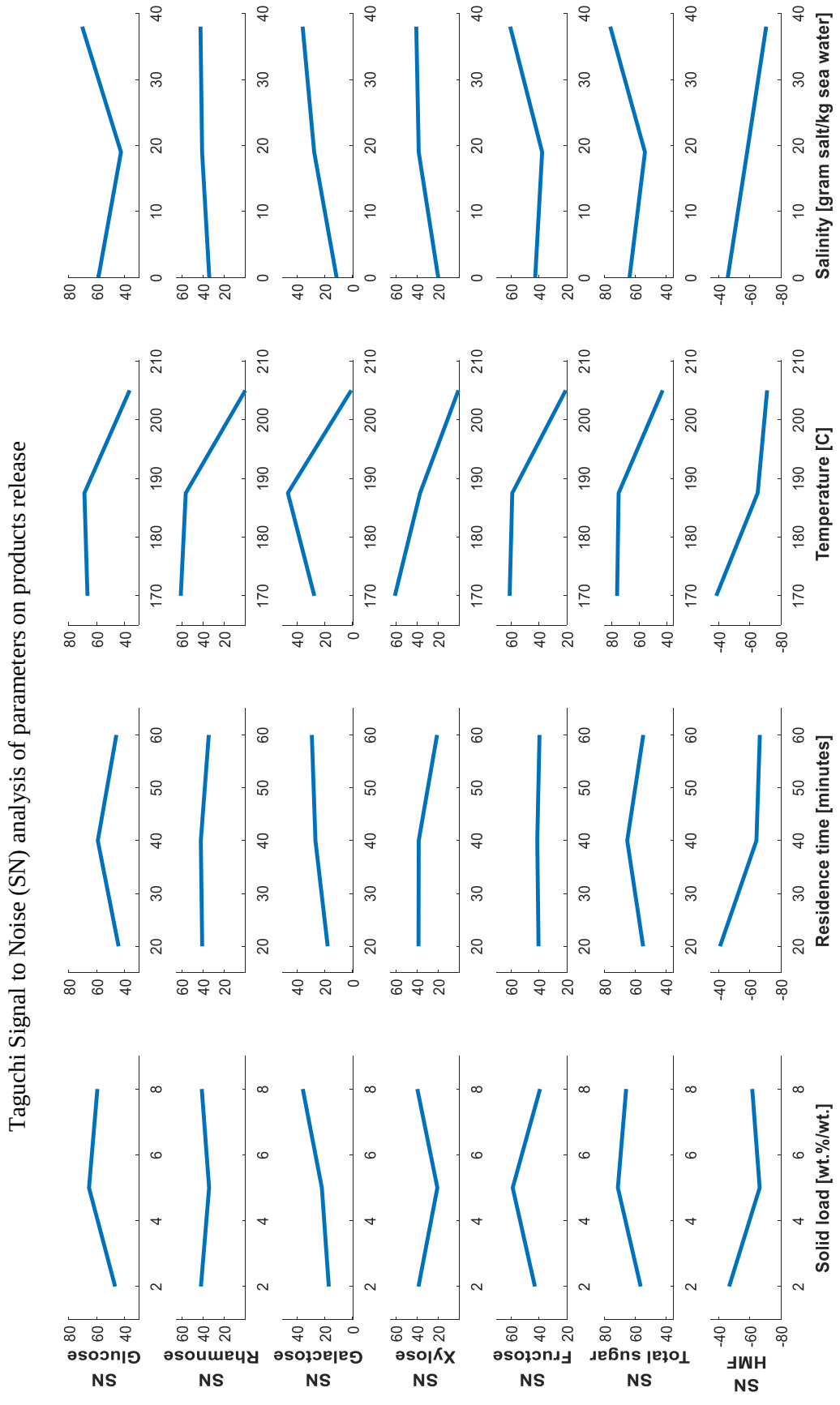

Figure 11- Taguchi Signal to Noise analysis

4.5 Mass Balance

At each experiment the solid residue mass was weighted. The solid residue comprises of the hydrochar and water-soluble solids. **Table 11** summarizes the solid mass recovery.

Note: During the residue extraction loses of solids occur (solids in sampling line, solids attached to stirrer etc.), thus resulting in an error. This error was not accurately quantified but is much larger (in orders of magnitude) than the mass scale error. This resulted in a high error with the 2 percent solid load experiments, thus these results are not reliable and are not shown. **Figure 12** shows the mass recovery of the experiments.

Table 11- Taguchi experiments solid mass recovery

Exp #	Hydrochar yield (wt.%/wt.)*	Water soluble yield (wt.%/wt.)*	Total solid yield (wt.%/wt.)*
2	20.5	58.0	78.5
11	14.4	77.7	92.1
3	16.4	61.4	77.9
12	22.4	55.0	77.4
5	14.1	62.4	76.5
14	21.4	45.4	66.8
6	22.4	60.7	83.1
15	25.5	49.3	74.8
8	5.5	70.8	76.2
17	4.5	76.9	81.4
9	14.5	58.2	72.7
18	14.5	54.5	69.0

*Mass recovered from initial algae dry mass

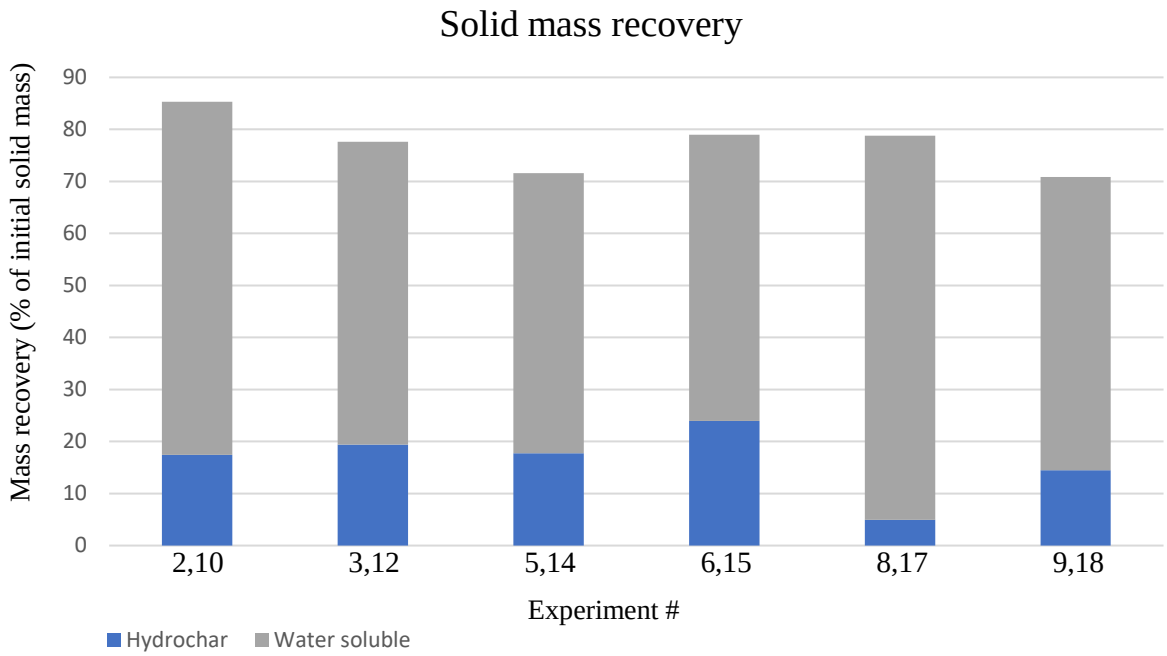

Figure 12- Taguchi experiments average solid residue mass recovery

The solid recovery is 71-85% of the initial biomass with hydrochar yields of 5-24%. The water-soluble solids include hydrolyzed carbohydrates fragments with different lengths, amino acids and soluble ash. The rest of the mass can be accounted to released algae moisture (**Table 12**), produced water due to the carbonization process and liquids formed in the process.

In experiments 3 and12 the hydrochar yield was 19.4%, the water-soluble solids yield is 58.2%, moisture that was released during the process (**Table 12**) comprises 19.1% and the rest (3.3%) can be attributed to produced water and volatile liquids.

4.6 Algae and hydrochar properties

The untreated algae and hydrochar from experiments 3,12 (**Figure 13**) were further examined. The ultimate, proximate, starch and HHV is summarized in the table below.

Table 12- Ulva biomass and hydrochar properties

		Untreated Algae	Hydrochar 170 ^{o}C, Solid Load 8% ,60 min, salinity 38 g/L
Ultimate (wt.%)	N	1.3	3.2
	C	23.8	43.3
	H	4.7	6.2
	S	5.1	1.2
	O	36	30.4
Proximate (wt.%)	Ash	29	15.5
	Moisture	20.6	7.5
Biochemical (wt.%)	Starch*	4.4	-
HHV (MJ kg^{-1})	Boie	10.5	19.4
	Grummel & Davis	9.6	18.7
	Measured value (Calorimeter)	10	20.2

*Dry weight basis

** the hydrochar properties is the average properties of experiment 3 and 12.

As predicted the hydrochar carbon content increased and oxygen content decreased compared to the original biomass due to the carbonization process thus increasing the HHV by 9-10 MJ (energy densification of 1.85-2) compared to the initial sample. The energy yield (energy densification multiplied by hydrochar yield) is 42-46%, similar to other carbonization studies on macroalgae which show 40-67% energy yield [31], [69], [70]. Arable biomass such as corn and sugarcane have higher reported energy yield of 68% (at 175^{o}C and 30 min residence time) [86].

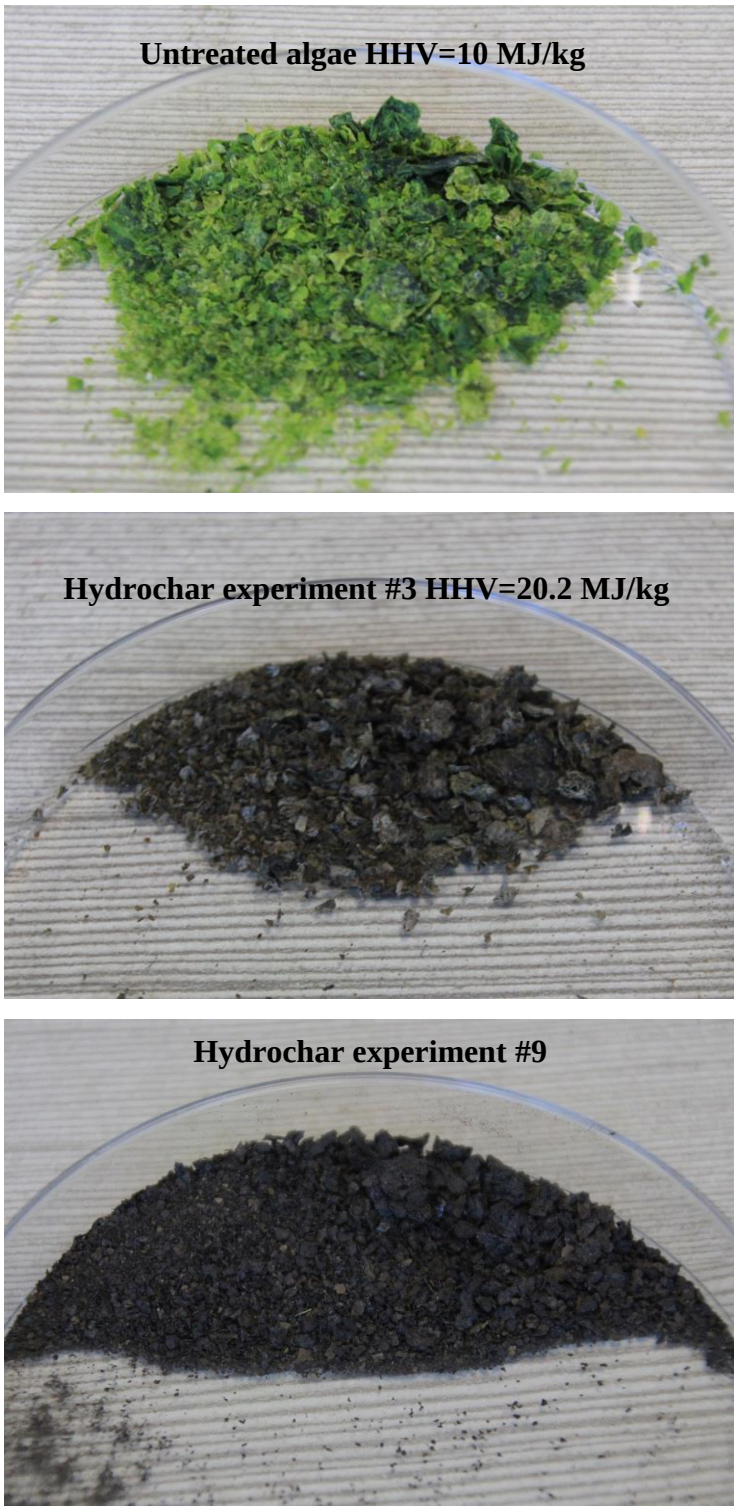

Figure 13- Algae and hydrochar images

5 Solar plant simulation

Using the results from Taguchi experiments 3 and 12, A simulation of combined solar electricity generation and fuel production cycle using Thermolib® toolbox for MATLAB® / Simulink® was made solving mass and energy balances. The configuration chosen (**Figure 14**) combines conventional technologies used today, other configurations could be also applied and studied. A mixture of water and algae (15% algae, 85% water) is pumped using high pressure pump into a pre-heater, then the mixture enters the reactor which is heated by a parabolic though that uses thermal oil (Therminol VP-1). After the reaction the slurry leaves the reactor into depressurized tank which separates the vapor and solid/aqueous phases. The solid char residue can be dried and combusted for energy production. The aqueous phase pre heats the feed, filtered and fermented to alcoholic fuel. The vapor from the depressurizing tank provides exchanges heat to the ORC heat transfer fluid, condenses and leaves as desalinated water. The solar heat transfer fluid also powers a steam turbine before heating the reactor.

A schematic diagram is shown below.

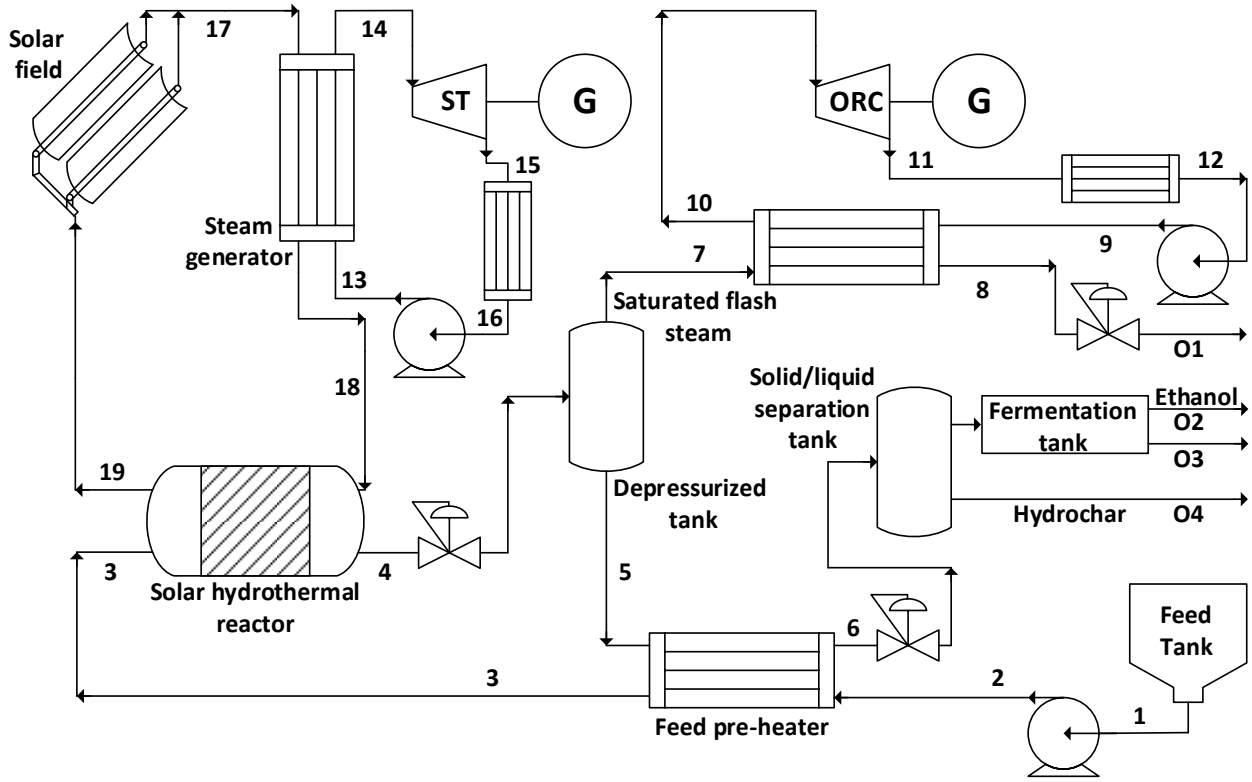

Figure 14- Schematic diagram of solar electricity and fuel production from algae

5.2 Simulation assumptions and input parameters

The assumptions for the simulation and input parameters are shown below and in **Table 13.**

- Steady state steady flow.
- No heat loses to the environment (heat exchangers, reactor, pipes).
- No pressure drops in the heat exchangers/condensers, pipes.
- C_p (algae water mixture) = C_p(water). Detailed calculation of the mixture heat capacity can be seen in Appendix 2.
- The heat for/from the chemical reactions is negligible (see Appendix 3).

Table 13- Simulation input parameters

Parameter	Value	Units
Pumps isentropic efficiencies	80	%
Turbines isentropic efficiencies	85	%
Collector efficiency (optical and thermal)	65	%
Biomass pump output pressure	7.87	bar
Flash steam pressure	2	bar
Solar steam turbine outlet pressure	0.05	bar
Steam turbine pump pressure	70	bar
ORC turbine outlet pressure	0.07	bar
Heat transfer rate to thermal oil	625	kW
Feed tank temperature	25	^{0}C
Thermal oil temperature at solar field outlet	376	^{0}C
Depressurized tank temperature	120	^{0}C
Solar steam turbine outlet temperature	32.8	^{0}C
ORC turbine outlet temperature	26.8	^{0}C
Biomass flow rate	1	kg· s^{-1}
ORC fluid flow rate	0.47	kg· s^{-1}
Steam turbine cycle flow rate	0.13	kg· s^{-1}
Thermal oil flow rate	1.1	kg· s^{-1}
Hydrothermal reactor heat exchanger effectiveness	0.9	
Pre-heater heat exchanger effectiveness	0.97	
Steam generator and ORC heat exchangers effectiveness	1	

5.3 Simulation outputs

Table 14 Summarizes all state points in the plant as shown the **Figure 14.**

Table 14- Simulation state points description

Point	Compound	Description	ṁ kg·s^{-1}	T ^{0}C	P bar	h kJ· kg^{-1}	H(kJ), Ḣ(kW)
1	Water	See **Table 16**	1	25	1	104.9	104.9
2	Water	See **Table 16**	1	25.2	7.87	105.8	105.8
3	Water	See **Table 16**	1	110	7.87	463.2	463.2
4	Water	See **Table 16**	1	170	7.87	718.9	718.9
5	Water	See **Table 16**	0.92	120	2	504.7	462.9
6	Water	See **Table 16**	0.92	27.4	2	115	105.5
7	Water (steam)	Pure	0.08	120	2	2705	224.6
8	Water	Pure	0.08	29.2	2	122.5	10.2
9	Isooctane	Pure	0.47	27	1.6	21.6	10.2
10	Isooctane	Pure	0.47	116.5	1.6	477.8	224.6
11	Isooctane	Pure	0.47	80	0.07	406.7	191.1
12	Isooctane	Pure	0.47	26.8	0.07	21.3	10
13	Water	Pure	0.13	35	70	146.5	18.5
14	Water (steam)	Pure	0.13	370	70	3072	387.2
15	Water (steam)	Pure	0.13	32.8	0.05	2015	254
16	water	Pure	0.13	32.8	0.05	137.8	17.4
17	VP-1	Pure	1.1	376	15	738.9	812
18	VP-1	Pure	1.1	232	15	403.2	443.1
19	VP-1	Pure	1.1	113	15	170.2	187

Using the simulation outputs, the steam and ORC turbines power blocks thermal efficiency was calculated using the following equation:

$$\eta = \frac{\dot{W}}{\dot{Q}} \tag{16}$$

Where Ẇ is the turbine power output and Q̇ is the input heat transfer flow to the power block.

The work of the steam and ORC turbines are the work transfer rate subtractions between state points 15-14 and 11-10, respectively. The heat inputs are the heat transfer rate subtraction between state points 14-13 and 10-9 for the steam turbine and ORC turbine, respectively. The resulting thermal efficiency of the steam turbine power block is 35% and a thermal efficiency of 15.6% obtained for the ORC power block.

The products output can be seen in **Table 15** with 83 $g \cdot s^{-1}$ of water, 0.7 $g \cdot s^{-1}$ ethanol and 29.1 $g \cdot s^{-1}$ hydrochar mass flow rate. Also, a 0.7 $g \cdot s^{-1}$ carbon dioxide is produced during the fermentation process.

Table 15- Simulation outputs mass fractions

Line	Output	Mass flow (g/s)
O1	Water*	83
O2	Ethanol**	0.7
O3	Brine	886.5
O4	Hydrochar	29.1

*Can contain some other liquids from organic volatiles (less than 0.5%).

**Assuming 50% sugar to ethanol conversion rate.

The detailed mass fraction based on the algae and hydrochar properties from experiments 3 and 12 can be seen in **Table 16.** It is notable that most of the ash was solubilized and the hydrochar moisture content decreased following the hydrothermal treatment.

Table 16- Detailed simulation mass composition

Point		1,2,3	4	5,6
Sea water flow (g/s)	Water	817.7	817.7	738
	Salts	32.3	32.3	32.3
Algae flow (g/s)	Moisture	31	2.2	2.2
	Ash	34.5	4.2	4.2
	Organic (non-soluble)	84.5	22.7	22.7
	Water from algae moisture	0	28.8	26
	Water soluble ash	0	30.3	30.3
	Water soluble compounds	0	57.2	57.2
	Volatiles and water due to carbonization	-	4.6	4.1
Algae	HHV(MJ/kg)	10	20.2	20.2
	LHV(MJ/kg)	9	19.2	19.2

The LHV was calculated using the following definition:

$$LHV = HHV - \Delta H_{vap} \cdot M_{H_2O} \quad (17)$$

Note: The hydrochar chemical formula was determined using the result from the elemental analysis.

5.4 System performance analysis

For our hybrid cycle two efficiencies were calculated, first law efficiency (η_I) and electrical efficiency (η_{el}) [87], [88] and described as follow:

$$\eta_I = \frac{\dot{W} + \dot{Q}_{fuel\_out}}{\dot{Q}_{fuel\_in} + \dot{Q}_{solar}} \tag{18}$$

Where in our case:

$$\dot{Q}_{fuel\_in} = \dot{m}_{algae} \cdot LHV_{algae} \tag{19}$$

$$\dot{Q}_{fuel\_out} = \dot{m}_{hydrochar} \cdot LHV_{hydrochar} + \dot{m}_{ethanol} \cdot LHV_{ethanol} \tag{20}$$

$$\dot{Q}_{solar} = \frac{\dot{Q}_{solar\_net}}{\eta_c} \tag{21}$$

$$\dot{W} = \dot{W}_{steam\_turbine} + \dot{W}_{ORC\_turbine} - \sum \dot{W}_{pumps} \tag{22}$$

State point 1 is the fuel input, the fuel outputs are outputs O2 and O4 in the scheme. $\dot{Q}_{solar}$ Is the total heat flow that the collector receives. $\dot{Q}_{solar\_net}$ is the net heat flow that the thermal oil receives (state points 17,19). As stated before the work of the steam and ORC turbines are the work transfer rate subtractions between state points 15-14 and 11-10, respectively. The pumps work inputs for the biomass pump, steam turbine cycle pump and ORC pump are the subtractions of the work transfer rate between state points 2-1, 13-16 and 9-12, respectively.

and the electrical efficiency:

$$\eta_{el} = \frac{\dot{W}}{\dot{Q}_{fuel\_in} + \dot{Q}_{solar}} \tag{23}$$

where in this case the fuel heat is converted to electricity.

In our case:

$$\dot{Q}_{fuel\_in} = 1070\ kW$$

$$\dot{Q}_{fuel\_out} = 516 + 19 = 535\ kW$$

And from simulation:

$$\dot{Q}_{solar\_net} = 625\ kW$$

$$\dot{Q}_{solar} = 961\ kW$$

$$\dot{W} = 133 + 33 - 2 = 164\ kW$$

$$\eta_I = 34.4\%$$

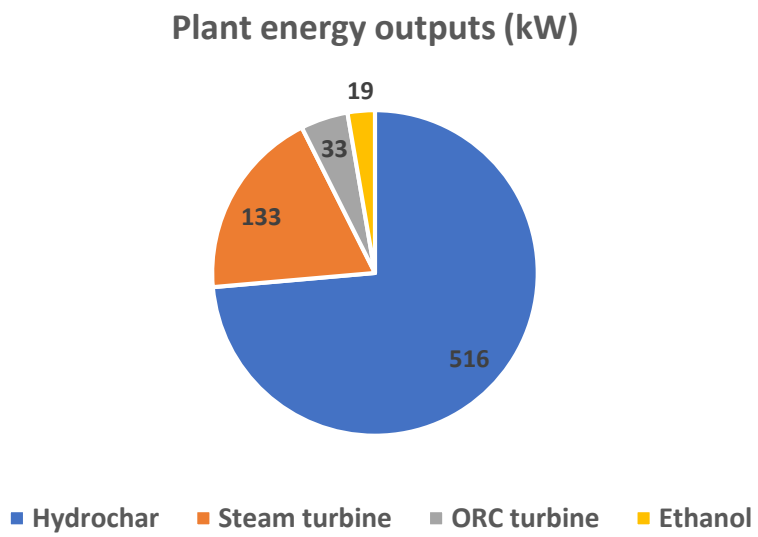

Figure 15- Solar plant energy (heat and power) outputs

As can be seen from **Figure 15** the contribution of the ethanol heat flow is neglectable compared to the hydrochar (19kW compared to 516 kW) and comprises only 3% of the net solar heat. It is notable that the ethanol and hydrochar heat flow is not thermodynamically equivalent to the work outputs of the turbines. Transforming the hydrochar and ethanol heat to electricity using modern coal power plant efficiency of 40% [89] will generate 206 kW and 7.6 kW from the hydrochar and ethanol, respectively, resulting in electrical efficiency of $\eta_{el} =$ 18.6%, similar to conventional parabolic trough solar power plants, in which the electrical efficiency can reach 20% [88], [90] and on the lower end comparing to studies conducted on biomass powered plants with electrical efficiencies of 18-36% [87], [91]. With these results the production of ethanol from algae via thermal hydrolysis is not attractive and optimizing the carbonization process is likely to give better plant performances.

Distilled water is also a product with a flow rate of 83 gram/s, equivalent to 300 liter/hour. The electricity saving compared to current reverse osmosis distillation plants (~3.5 kWh/m^3) [92] is negligible and accounts for 1kW.

6 Summary and conclusions

This work includes detailed analysis of major parameters effect on all released monosaccharide in a thermal hydrolysis process with temperature has the highest effect on the hydrolysis process followed by salinity, then solid load and residence time. chemical and enzymatic hydrolysis conducted on *Ulva* biomass show higher yields than thermal hydrolysis conducted in this study. Glucose was the major released monosaccharide at the tested conditions with maximum yield of 4.92 mg/g dry algae. The maximum sugar yield obtained in this study was 9.34 mg sugars/g dry algae obtained at 170^{o}C, 8% solid load, 60 min residence time and 100% salinity.

Combining solar energy as a heat source for deconstruction of biomass was also studied. The resulted ethanol heat flow that can be achieved from thermal hydrolysis is negligible compared to the hydrochar heat flow, thus, optimizing the carbonization process energy yield should give us better results and higher biomass to power conversion efficiencies. With this study results unless much higher algae sugar content could be achieved from the downstream process which will results in higher monosaccharide yields per a biomass unit, ethanol production via thermal hydrolysis using parabolic through technology is not attractive.

For future work, the differences between thermal hydrolysis of the same compound from different biomasses (starch for example) and the reasons for the differences should be studied as it is not fully understood. With this said the effect of the biomass structure and biochemical compounds on the hydrolysis and carbonization of each compound separately is also not fully understood.

By thermally hydrolyzing the all biomass ingredients which could have been used for different purposes are destroyed, a study should be made on integration, feasibility and effectiveness of a process initially separating the biomass compounds (cellulose, proteins etc.) and using them for a desired process, this will give a better usage of the biomass and will result in a higher yield for each process separately.

7 References

[1] "Conti, John, Holtberg, Paul, Diefenderfer, Jim, LaRose, Angelina, Turnure, James T., & Westfall, Lynn. International Energy Outlook 2016 With Projections to 2040. United States."

[2] J. Popp, Z. Lakner, M. Harangi-Rákos, and M. Fári, "The effect of bioenergy expansion: Food, energy, and environment," *Renew. Sustain. Energy Rev.*, vol. 32, pp. 559–578, 2014.

[3] C. M. Duarte *et al.*, "Will the Oceans Help Feed Humanity?," *Bioscience*, vol. 59, no. 11, pp. 967–976, 2009.

[4] F. Fernand, A. Israel, J. Skjermo, T. Wichard, K. R. Timmermans, and A. Golberg, "Offshore macroalgae biomass for bioenergy production: Environmental aspects, technological achievements and challenges," *Renew. Sustain. Energy Rev.*, no. October, 2017.

[5] E. Vitkin, A. Golberg, and Z. Yakhini, "BioLEGO — a web-based application for biorefinery design and evaluation of serial biomass fermentation," *TECHNOLOGY*, pp. 1–10, Jun. 2015.

[6] I. S. Tan, M. K. Lam, and K. T. Lee, "Hydrolysis of macroalgae using heterogeneous catalyst for bioethanol production," *Carbohydr. Polym.*, vol. 94, no. 1, pp. 561–566, 2013.

[7] J. M. Prado, R. Vardanega, M. A. Rostagno, T. Forster-Carneiro, and M. Angela, "The study of model systems subjected to sub- and supercritical water hydrolysis for the production of fermentable sugars," *Green Chem. Lett. Rev.*, vol. 8, no. 1, pp. 16–30, 2015.

[8] A. Meillisa, H.-C. Woo, and B.-S. Chun, "Production of monosaccharides and bio-active compounds derived from marine polysaccharides using subcritical water hydrolysis," *Food Chem.*, vol. 171, pp. 70–77, 2015.

[9] A. G. Roesijadi, A. Copping, and M. Huesemann, "Techno-Economic Feasibility Analysis of Offshore Seaweed Farming for Bioenergy and Biobased Products," 2008.

[10] P. Eva, G. Halfdan, M. N. Q., and H. Bärbel, "Main and interaction effects of acetic acid, furfural, and p-hydroxybenzoic acid on growth and ethanol productivity of yeasts," *Biotechnol. Bioeng.*, vol. 63, no. 1, pp. 46–55, Mar. 2000.

[11] R. Roberto and S. Ferdi, "Acid Hydrolysis of Cellulose as the Entry Point into

Biorefinery Schemes," *ChemSusChem*, vol. 2, no. 12, pp. 1096–1107.

[12] R. Jiang, K. N. K. N. Ingle, and A. Golberg, "Macroalgae (seaweed) for liquid transportation biofuel production: what is next?," *Algal Res.*, vol. 14, pp. 48–57, Mar. 2016.

[13] Q. Al Abdallah, B. T. Nixon, and J. R. Fortwendel, "The Enzymatic Conversion of Major Algal and Cyanobacterial Carbohydrates to Bioethanol," *Front. Energy Res.*, vol. 4, no. November, pp. 1–15, 2016.

[14] N. Schultz-Jensen *et al.*, "Pretreatment of the macroalgae Chaetomorpha linum for the production of bioethanol - Comparison of five pretreatment technologies," *Bioresour. Technol.*, vol. 140, pp. 36–42, 2013.

[15] N. Ben Yahmed, M. A. Jmel, M. Ben Alaya, H. Bouallagui, M. N. Marzouki, and I. Smaali, "A biorefinery concept using the green macroalgae Chaetomorpha linum for the coproduction of bioethanol and biogas," *Energy Convers. Manag.*, vol. 119, pp. 257–265, 2016.

[16] D. Klein-Marcuschamer, P. Oleskowicz-Popiel, B. A. Simmons, and H. W. Blanch, "The challenge of enzyme cost in the production of lignocellulosic biofuels," *Biotechnol. Bioeng.*, vol. 109, no. 4, pp. 1083–1087, 2012.

[17] Z.-Y. Sun, Y.-Q. Tang, S. Morimura, and K. Kida, "Reduction in environmental impact of sulfuric acid hydrolysis of bamboo for production of fuel ethanol," *Bioresour. Technol.*, vol. 128, pp. 87–93, 2013.

[18] R. Jiang, Y. Linzon, E. Vitkin, Z. Yakhini, A. Chudnovsky, and A. Golberg, "Thermochemical hydrolysis of macroalgae Ulva for biorefinery: Taguchi robust design method," *Sci. Rep.*, vol. 6, no. 1, p. 27761, Sep. 2016.

[19] M. F. Rosa *et al.*, "Cellulose nanowhiskers from coconut husk fibers: Effect of preparation conditions on their thermal and morphological behavior," *Carbohydr. Polym.*, vol. 81, no. 1, pp. 83–92, 2010.

[20] M. Möller, P. Nilges, F. Harnisch, and U. Schröder, "Subcritical water as reaction environment: Fundamentals of hydrothermal biomass transformation," *ChemSusChem*, vol. 4, no. 5. pp. 566–579, 2011.

[21] S. S. Toor, L. Rosendahl, and A. Rudolf, "Hydrothermal liquefaction of biomass: A review of subcritical water technologies," *Energy*, vol. 36, no. 5. pp. 2328–2342, 2011.

[22] M. J. Cocero *et al.*, "Understanding biomass fractionation in subcritical & supercritical water," *J. Supercrit. Fluids*, vol. 133, pp. 550–565, Mar. 2018.

[23] T. M. Mata, A. A. Martins, and N. S. Caetano, "Microalgae for biodiesel production and

other applications: A review," *Renew. Sustain. Energy Rev.*, vol. 14, no. 1, pp. 217–232, 2010.

[24] D. L. Barreiro, W. Prins, F. Ronsse, and W. Brilman, "Hydrothermal liquefaction (HTL) of microalgae for biofuel production: State of the art review and future prospects," *Biomass and Bioenergy*, vol. 53, pp. 113–127, 2013.

[25] A. Robin, P. Chavel, A. Chemodanov, A. Israel, and A. Golberg, "Diversity of monosaccharides in marine macroalgae from the Eastern Mediterranean Sea," *Algal Res.*, vol. 28, pp. 118–127, 2017.

[26] Y. Lehahn, K. N. Ingle, and A. Golberg, "Global potential of offshore and shallow waters macroalgal biorefineries to provide for food, chemicals and energy: feasibility and sustainability," *Algal Res.*, vol. 17, pp. 150–160, 2016.

[27] P. Bikker *et al.*, "Biorefinery of the green seaweed Ulva lactuca to produce animal feed, chemicals and biofuels," *J. Appl. Phycol.*, vol. 28, pp. 3511–3525, 2016.

[28] A. Chemodanov *et al.*, "Net primary productivity, biofuel production and CO2 emissions reduction potential of Ulva sp. (Chlorophyta) biomass in a coastal area of the Eastern Mediterranean," *Energy Convers. Manag.*, vol. 148, pp. 1497–1507, 2017.

[29] T. Potts, J. Du, M. Paul, P. May, R. Beitle, and J. Hestekin, "The production of butanol from Jamaica bay macro algae," in *Environmental Progress and Sustainable Energy*, 2012, vol. 31, pp. 29–36.

[30] H. van der Wal, B. L. H. M. H. M. Sperber, B. Houweling-Tan, R. R. C. C. Bakker, W. Brandenburg, and A. M. López-Contreras, "Production of acetone, butanol, and ethanol from biomass of the green seaweed Ulva lactuca," *Bioresour. Technol.*, vol. 128, pp. 431–437, 2013.

[31] S. Daneshvar, F. Salak, T. Ishii, and K. Otsuka, "Application of Subcritical Water for Conversion of Macroalgae to Value-Added Materials," *Ind. Eng. Chem. Res.*, vol. 51, no. 1, pp. 77–84, 2012.

[32] N. Neveux *et al.*, "Biocrude yield and productivity from the hydrothermal liquefaction of marine and freshwater green macroalgae," *Bioresour. Technol.*, vol. 155, no. Supplement C, pp. 334–341, 2014.

[33] W.-Y. Choi, D.-H. Kang, and H.-Y. Lee, "Enhancement of the saccharification yields of Ulva pertusa kjellmann and rape stems by the high-pressure steam pretreatment process," *Biotechnol. Bioprocess Eng.*, vol. 18, no. 4, pp. 728–735, Aug. 2013.

[34] D. Zhou, L. Zhang, S. Zhang, H. Fu, and J. Chen, "Hydrothermal Liquefaction of Macroalgae Enteromorpha prolifera to Bio-oil," *Energy & Fuels*, vol. 24, no. 7, pp.

4054–4061, 2010.

[35] D. Rodrigues *et al.*, “Chemical composition of red, brown and green macroalgae from Buarcos bay in Central West Coast of Portugal,” *Food Chem.*, vol. 183, pp. 197–207, 2015.

[36] P. Chermapandi, S. C, G. Karthik, A. Hemalatha, M. Suresh, and P. Anantharaman, “Biochemical composition of some selected seaweeds from Tuticorin coast,” *Adv. Appl. Sci. Res.*, vol. 4, pp. 362–366, 2013.

[37] N. J. Kim, H. Li, K. Jung, H. N. Chang, and P. C. Lee, “Ethanol production from marine algal hydrolysates using Escherichia coli KO11,” *Bioresour. Technol.*, vol. 102, no. 16, pp. 7466–7469, 2011.

[38] G. J. de Moraes Rocha, V. M. Nascimento, A. R. Gonçalves, V. F. N. Silva, and C. Martín, “Influence of mixed sugarcane bagasse samples evaluated by elemental and physical–chemical composition,” *Ind. Crops Prod.*, vol. 64, pp. 52–58, 2015.

[39] X. P. Ye, L. Liu, D. Hayes, A. Womac, K. Hong, and S. Sokhansanj, “Fast classification and compositional analysis of cornstover fractions using Fourier transform near-infrared techniques,” *Bioresour. Technol.*, vol. 99, no. 15, pp. 7323–7332, 2008.

[40] I. C. and J. J. H. Lei, “Hydrothermal Pretreatment of Lignocellulosic Biomass and Kinetics,” *J. Sustain. Bioenergy Syst.*, vol. Vol. 3, no. No. 4, pp. 250–259, 2013.

[41] L. Ramos, E. M. Kristenson, and U. A. T. Brinkman, “Current use of pressurised liquid extraction and subcritical water extraction in environmental analysis,” *J. Chromatogr. A*, vol. 975, no. 1, pp. 3–29, 2002.

[42] A. Kruse and E. Dinjus, “Hot compressed water as reaction medium and reactant: Properties and synthesis reactions,” *J. Supercrit. Fluids*, vol. 39, no. 3, pp. 362–380, 2007.

[43] W. L. Marshall and E. U. Franck, “Ion product of water substance, 0–1000 °C, 1–10,000 bars New International Formulation and its background,” *J. Phys. Chem. Ref. Data*, vol. 10, no. 2, pp. 295–304, 1981.

[44] M. Maria, N. Peter, H. Falk, and S. Uwe, “Subcritical Water as Reaction Environment: Fundamentals of Hydrothermal Biomass Transformation,” *ChemSusChem*, vol. 4, no. 5, pp. 566–579.

[45] S. R. Logan, “The origin and status of the Arrhenius equation,” *J. Chem. Educ.*, vol. 59, no. 4, p. 279, Apr. 1982.

[46] Y. Chen *et al.*, “Thermochemical conversion of low-lipid microalgae for the production of liquid fuels: challenges and opportunities,” *RSC Adv.*, vol. 5, no. 24, pp. 18673–

18701, 2015.

[47] T. Rogalinski, K. Liu, T. Albrecht, and G. Brunner, “Hydrolysis kinetics of biopolymers in subcritical water,” *J. Supercrit. Fluids*, vol. 46, no. 3, pp. 335–341, 2008.

[48] S. Mitsuru, A. Tadafumi, and A. Kunio, “Kinetics of cellulose conversion at 25 MPa in sub- and supercritical water,” *AIChE J.*, vol. 50, no. 1, pp. 192–202.

[49] T. Gagić, A. Perva-Uzunalić, Ž. Knez, and M. Škerget, “Hydrothermal Degradation of Cellulose at Temperature from 200 to 300 °C,” *Ind. Eng. Chem. Res.*, vol. 57, no. 18, pp. 6576–6584, 2018.

[50] N. Makiko and F. Toshitaka, “Glucose production by hydrolysis of starch under hydrothermal conditions,” *J. Chem. Technol. Biotechnol.*, vol. 79, no. 3, pp. 229–233.

[51] C. D. R., L. Y. Y., and C. R. P., “Modeling of percolation process in hemicellulose hydrolysis,” *Biotechnol. Bioeng.*, vol. 25, no. 1, pp. 3–17.

[52] B. Nandan, M. D. G., and B. N. N., “Kinetic studies of corn stover saccharification using sulphuric acid,” *Biotechnol. Bioeng.*, vol. 26, no. 4, pp. 320–327.

[53] N. Trivedi, V. Gupta, C. R. K. Reddy, and B. Jha, “Enzymatic hydrolysis and production of bioethanol from common macrophytic green alga Ulva fasciata Delile,” *Bioresour. Technol.*, vol. 150, pp. 106–112, Dec. 2013.

[54] D. Vasic-Racki, “History of industrial biotransformations—dreams and realities,” *Ind. biotransformations*, pp. 1--35, 2006.

[55] P. J. Chambers and I. S. Pretorius, “Fermenting knowledge: the history of winemaking, science and yeast research,” *EMBO Rep.*, vol. 11, no. 12, pp. 914–920, 2010.

[56] F. W. Bai, W. A. Anderson, and M. Moo-Young, “Ethanol fermentation technologies from sugar and starch feedstocks,” *Biotechnol. Adv.*, vol. 26, no. 1, pp. 89–105, 2008.

[57] A. B. Diaz, A. Blandino, and I. Caro, “Value added products from fermentation of sugars derived from agro-food residues,” *Trends Food Sci. Technol.*, vol. 71, pp. 52–64, 2018.

[58] N. Trivedi, C. R. K. Reddy, R. Radulovich, and B. Jha, “Solid state fermentation (SSF)-derived cellulase for saccharification of the green seaweed Ulva for bioethanol production,” *Algal Res.*, vol. 9, pp. 48–54, 2015.

[59] H.-J. Huang, S. Ramaswamy, U. W. Tschirner, and B. V Ramarao, “A review of separation technologies in current and future biorefineries,” *Sep. Purif. Technol.*, vol. 62, no. 1, pp. 1–21, 2008.

[60] S. I. Mussatto *et al.*, “Technological trends, global market, and challenges of bio-ethanol production,” *Biotechnol. Adv.*, vol. 28, no. 6, pp. 817–830, 2010.

[61] J. R. M. Almeida, T. Modig, A. Petersson, B. Hähn-Hägerdal, G. Lidén, and M. F.

Gorwa-Grauslund, “Increased tolerance and conversion of inhibitors in lignocellulosic hydrolysates by Saccharomyces cerevisiae,” *Journal of Chemical Technology and Biotechnology*, vol. 82, no. 4. pp. 340–349, 2007.

[62] D. Heer and U. Sauer, “Identification of furfural as a key toxin in lignocellulosic hydrolysates and evolution of a tolerant yeast strain,” *Microb. Biotechnol.*, vol. 1, no. 6, pp. 497–506, 2008.

[63] F. C. R. Bergius, *Anwendung hoher Drucke bei chemischen Vorgängen und die Nachbildung des Entstehungsprozesses der Steinkohle*. Halle a.S., Knapp, 1913.

[64] J. Libra *et al.*, “Hydrothermal carbonization of biomass residuals: a comparative review of the chemistry, processes and applications of wet and dry pyrolysis,” *Biofuels*, 2011.

[65] Hans-Günter Ramke, “RAMKE, H.-G.; BLÖHSE, D.; LEHMANN, H.-J.; FETTIG, J., 2009: Hydrothermal Carbonization of Organic Waste in: COSSU, R.; DIAZ, L. F.; STEGMANN, R. (EDTS.), 2009: Sardinia 2009: Twelfth International Waste Management and Landfill Symposium, Sardinia, Italy,” 2009.

[66] M.-M. Titirici, A. Thomas, and M. Antonietti, “Back in the black: Hydrothermal carbonization of plant material as an efficient chemical process to treat the CO2 problem?,” *New J. Chem.*, vol. 31, 2007.

[67] “Hydrothermal Carbonization of Biomass for Energy and Crop Production ,” *Applied Bioenergy* , vol. 1. 2014.

[68] T. Wang, Y. Zhai, Y. Zhu, C. Li, and G. Zeng, “A review of the hydrothermal carbonization of biomass waste for hydrochar formation: Process conditions, fundamentals, and physicochemical properties,” *Renew. Sustain. Energy Rev.*, vol. 90, pp. 223–247, 2018.

[69] A. M. Smith and A. B. Ross, “Production of bio-coal, bio-methane and fertilizer from seaweed via hydrothermal carbonisation,” *Algal Res.*, vol. 16, no. Supplement C, pp. 1–11, 2016.

[70] Q. Xu, Q. Qian, A. Quek, N. Ai, G. Zeng, and J. Wang, “Hydrothermal Carbonization of Macroalgae and the Effects of Experimental Parameters on the Properties of Hydrochars,” *ACS Sustain. Chem. Eng.*, vol. 1, no. 9, pp. 1092–1101, 2013.

[71] Z. Liu, A. Quek, S. K. Hoekman, M. P. Srinivasan, and R. Balasubramanian, “Thermogravimetric investigation of hydrochar-lignite co-combustion,” *Bioresour. Technol.*, vol. 123, pp. 646–652, 2012.

[72] S. Mekhilef, R. Saidur, and A. Safari, “A review on solar energy use in industries,” *Renew. Sustain. Energy Rev.*, vol. 15, no. 4, pp. 1777–1790, 2011.

[73] Y. Tian and C. Y. Zhao, “A review of solar collectors and thermal energy storage in solar thermal applications,” *Appl. Energy*, vol. 104, pp. 538–553, 2013.

[74] M. Liu *et al.*, “Review on concentrating solar power plants and new developments in high temperature thermal energy storage technologies,” *Renew. Sustain. Energy Rev.*, vol. 53, pp. 1411–1432, 2016.

[75] P. Lichty, C. Perkins, B. Woodruff, C. Bingham, and A. Weimer, “Rapid High Temperature Solar Thermal Biomass Gasification in a Prototype Cavity Reactor,” *J. Sol. Energy Eng.*, vol. 132, no. 1, pp. 11012–11017, Jan. 2010.

[76] B. J. Hathaway, J. H. Davidson, and D. B. Kittelson, “Solar Gasification of Biomass: Kinetics of Pyrolysis and Steam Gasification in Molten Salt,” *J. Sol. Energy Eng.*, vol. 133, no. 2, pp. 21011–21019, Apr. 2011.

[77] R. Adinberg, M. Epstein, and J. Karni, “Solar Gasification of Biomass: A Molten Salt Pyrolysis Study,” *J. Sol. Energy Eng.*, vol. 126, no. 3, pp. 850–857, Jul. 2004.

[78] A. Giaconia *et al.*, “Biorefinery process for hydrothermal liquefaction of microalgae powered by a concentrating solar plant: A conceptual study,” *Appl. Energy*, vol. 208, pp. 1139–1149, 2017.

[79] A. Chemodanov, A. Robin, and A. Golberg, “Design of marine macroalgae photobioreactor integrated into building to support seagriculture for biorefinery and bioeconomy,” *Bioresour. Technol.*, vol. 241, pp. 1084–1093, 2017.

[80] R. S. Rao, C. G. Kumar, R. S. Prakasham, and P. J. Hobbs, “The Taguchi methodology as a statistical tool for biotechnological applications: A critical appraisal,” *Biotechnology Journal*, vol. 3. pp. 510–523, 2008.

[81] K. Mason, D.M. & Gandhi, “FORMULAS FOR CALCULATING THE HEATING VALUE OF COAL AND COAL CHAR: DEVELOPMENT, TESTS AND USES.” 1980.

[82] H. Yaich, H. Garna, S. Besbes, M. Paquot, C. Blecker, and H. Attia, “Chemical composition and functional properties of Ulva lactuca seaweed collected in Tunisia,” *Food Chem.*, vol. 128, pp. 895–901, 2011.

[83] J. Love, W. Mackie, J. W. Mckinnell, and E. Percival, “Starch-type polysaccharides isolated from the green seaweeds, enteromorpha compressa, ulva lactuca, cladophora rupestris, codium fragile, and chaetomorpha capillaris,” *J. Chem. Soc.*, pp. 4248–4256, 1963.

[84] S. Peleteiro, G. Garrote, V. Santos, and J. C. Parajó, “Conversion of hexoses and pentoses into furans in an ionic liquid,” *Afinidad*, vol. 71, no. 567, pp. 202–206, 2014.

[85] J. B. Binder and R. T. Raines, “Fermentable sugars by chemical hydrolysis of biomass,” *Proc. Natl. Acad. Sci.*, vol. 107, no. 10, pp. 4516–4521, 2010.

[86] S. K. Hoekman, A. Broch, C. Robbins, B. Zielinska, and L. Felix, “Hydrothermal carbonization (HTC) of selected woody and herbaceous biomass feedstocks,” *Biomass Convers. Biorefinery*, vol. 3, no. 2, pp. 113–126, Jun. 2013.

[87] C. Lythcke-Jørgensen, F. Haglind, and L. R. Clausen, “Exergy analysis of a combined heat and power plant with integrated lignocellulosic ethanol production,” *Energy Convers. Manag.*, vol. 85, pp. 817–827, 2014.

[88] E. J. Sheu, A. Mitsos, A. A. Eter, E. M. A. Mokheimer, M. A. Habib, and A. Al-Qutub, “A Review of Hybrid Solar–Fossil Fuel Power Generation Systems and Performance Metrics,” *J. Sol. Energy Eng.*, vol. 134, no. 4, pp. 41006–41017, Jul. 2012.

[89] A. G. Tumanovskii *et al.*, “Review of the coal-fired, over-supercritical and ultra-supercritical steam power plants,” *Therm. Eng.*, vol. 64, no. 2, pp. 83–96, Feb. 2017.

[90] P. Viebahn, Y. Lechon, and F. Trieb, “The potential role of concentrated solar power (CSP) in Africa and Europe—A dynamic assessment of technology development, cost development and life cycle inventories until 2050,” *Energy Policy*, vol. 39, no. 8, pp. 4420–4430, 2011.

[91] H. Liu, X. Yin, and C. Wu, “Comparative Evaluation of Biomass Power Generation Systems in China Using Hybrid Life Cycle Inventory Analysis,” *Sci. World J.*, vol. 2014, p. 735431, Oct. 2014.

[92] S. S. Shenvi, A. M. Isloor, and A. F. Ismail, “A review on RO membrane technology: Developments and challenges,” *Desalination*, vol. 368, pp. 10–26, 2015.

[93] A. Robin, M. Sack, A. Israel, W. Frey, G. Müller, and A. Golberg, “Deashing macroalgae biomass by pulsed electric field treatment,” *Bioresour. Technol.*, vol. 255, pp. 131–139, 2018.

[94] D. R. Lide, *CRC Handbook of Chemistry and Physics*. .

[95] D. T. Jamieson, J. S. Tudhope, R. Morris, and G. Cartwright, “Physical properties of sea water solutions: heat capacity,” *Desalination*, vol. 7, no. 1, pp. 23–30, 1969.

[96] P. Bösch, A. Modarresi, and A. Friedl, “Comparison of combined ethanol and biogas polygeneration facilities using exergy analysis,” *Appl. Therm. Eng.*, vol. 37, pp. 19–29, 2012.

Appendix 1- Taguchi Signal to Noise calculations

Table A1. Calculated signal-to-noise (SN) ratios for measured parameters and their ranking in importance for glucose release.

Level	T (℃)	Time (min)	Solid load (%)	Salinity (%)
1	66.7	44.4	46.9	58.9
2	68.9	59.3	65.6	42.7
3	36.5	46.0	59.6	70.5
Δ	32.5	14.9	18.7	27.8
Rank	1	4	3	2

Table A2. Calculated signal-to-noise (SN) ratios for measured parameters and their ranking in importance for rhamnose release.

Level	T (℃)	Time (min)	Solid load (%)	Salinity (%)
1	60.9	40.7	41.9	34.0
2	56.2	42.0	34.2	40.8
3	0.0	34.5	41.1	42.3
Δ	60.9	7.5	7.7	8.3
Rank	1	4	3	2

Table A3. Calculated signal-to-noise (SN) ratios for measured parameters and their ranking in importance for galactose release.

Level	T (℃)	Time (min)	Solid load (%)	Salinity (%)
1	27.5	17.9	17.1	11.5
2	46.5	26.7	22.1	27.6
3	1.0	29.3	35.8	35.9
Δ	45.5	11.4	18.7	24.5
Rank	1	4	3	2

Table A4. Calculated signal-to-noise (SN) ratios for measured parameters and their ranking in importance for xylose release.

Level	T (℃)	Time (min)	Solid load (%)	Salinity (%)
1	60.9	38.6	38.6	20.0
2	37.1	38.4	20.8	38.4
3	1.0	21.1	39.7	40.7
Δ	59.9	17.4	18.8	20.7
Rank	1	4	3	2

Table A5. Calculated signal-to-noise (SN) ratios for measured parameters and their ranking in importance for fructose release.

Level	T (℃)	Time (min)	Solid load (%)	Salinity (%)
1	61.0	40.3	42.9	42.7
2	59.1	41.2	58.8	37.7
3	20.8	39.6	39.2	60.6
Δ	40.2	1.7	19.6	22.9
Rank	1	4	3	2

Table A6. Calculated signal-to-noise (SN) ratios for measured parameters and their ranking in importance for HMF production.

Level	T (℃)	Time (min)	Solid load (%)	Salinity (%)
1	-38.3	-40.7	-46.6	-45.7
2	-65.0	-64.2	-66.3	-58.2
3	-71.1	-66.4	-61.5	-70.5
Δ	32.8	25.7	19.7	24.8
Rank	1	2	4	3

Table A7. Calculated signal-to-noise (SN) ratios for measured parameters and their ranking in importance for total sugar yield production.

Level	T (°C)	Time (min)	Solid load (%)	Salinity (%)
1	75.9	54.8	56.4	63.7
2	74.8	65.2	71.3	53.6
3	42.8	54.7	65.9	76.3
Δ	33.1	10.5	14.9	22.7
Rank	1	4	3	2

Table A8. Optimum process conditions for maximum monosaccharide release and minimum HMF production by subcritical water hydrolysis in the range of parameters as defined in Table 2.

	T (°C)	Time (min)	Solid load (%)	Salinity (%)
Rhamnose	170	40	2	100
Galactose	187	60	8	100
Glucose	187	40	8	100
Xylose	170	20	8	100
Fructose	170	40	5	100
HMF	170	20	2	0
Total monosaccharides	170	40	5	100

Appendix 2- heat capacity of algae and water mixture

Calculation of algae and sea water heat capacity (at 25℃) was made using **equation A1**

$$C_P(mixture) = \sum_i y_i \cdot C_{P,i} \quad \text{(A1)}$$

Where y_i is the mass fraction of component i and $C_{P,i}$ is the heat capacity of component i.

First the algae ash heat capacity was calculated using *Ulva* ash composition taken from [93].

Table A9. Algae ash composition

Compound	Mass fraction	Cp($kJ \cdot kg^{-1} \cdot K^{-1}$)
S	25.4	0.71
NaCl	34.7	0.86
Mg	18.6	1.02
P	1.1	0.77
K	11.5	0.75
Ca	8.7	0.65

Heat capacities of the ash compounds were taken from [94]

The heat capacity obtained is Cp(ash)=0.82 ($kJ \cdot kg^{-1} \cdot K^{-1}$)

The algae heat capacity was calculated using the following algae composition

Table A10. Algae proximate and biochemical composition

Compound	Mass fraction %	Cp($kJ \cdot kg^{-1} \cdot K^{-1}$)	Ref.
Ash	23	0.82	-
moisture	20.6	4.18	[95]
Protein*	16.5	1.3	[96]
Carbohydrate*	34.7	1.28	[96]
Lipid*	5.2	2.06	[96]

*Estimation using the average composition from **Table 1**

Obtaining Cp(algae)=1.81 ($kJ \cdot kg^{-1} \cdot K^{-1}$)

Sea water heat capacity (3.8% salts) was taken from [95] and equals:

Cp (sea water) =3.98 ($kJ \cdot kg^{-1} \cdot K^{-1}$). Giving us a total mixture (85% sea water and 15% algae) heat capacity of:

Cp (mixture)=3.66 ($kJ \cdot kg^{-1} \cdot K^{-1}$)

The heat capacity differs by 12% from pure water which used in the simulation.

Appendix 3- heat for/from hydrothermal reactions

To justify the neglection of the heat needed/obtained from the hydrolysis and carbonization reactions the following calculation were made:

Carbonization reactions can be described by:

$$(C_6H_{12}O_5)_4 \rightarrow C_{21}H_{16}O_2 + 3CO_2 + 12H_2O\ ;\ \Delta H_R = -297.9\frac{kJ}{mol}$$

$$C_6H_{12}O_6 \rightarrow C_6H_2O + 5H_2O\ ;\ \Delta H_R = -1040\frac{kJ}{mol}$$

$$C_6H_{12}O_6 \rightarrow C_6H_4O_2 + 4H_2O\ ;\ \Delta H_R = -950\frac{kJ}{mol}$$

Since the algae moisture and ash content sums to 43.6% The rest can potentially undergo carbonization. If we assume that all the rest of the mass (56.4%=84.5 gram) are carbohydrates that will fully undergo carbonization, the maximum heat produced from the reactions accounts for only 0.13kW compared to 256kW exchanged in the reactor.

Same calculation for the hydrolysis process:

$$C_6H_{10}O_5 + H_2O \rightarrow C_6H_{12}O_6\ ;\ \Delta H_R = -22\frac{kJ}{mol} \qquad \text{(A2)}$$

The maximum produced heat from the hydrolysis process accounts for $3.9\cdot10^{-3}$ kW.

Appendix 4- *Cladophora* experiments

In this series of experiments, a different green macroalgae *Cladophora* was taken as the biomass. The effect of the residence time is investigated (i.e. finding the time at which the sugar yield is maximal). The solid load, salinity and temperature were constant. Also, a catalyst (cobalt chloride) was added to attempt increase sugar yield.

4 experiments were made. In each experiment the reactor was inserted with 8 grams of algae and:

Experiment #1 92ml of sea water (3.8% salinity)

Experiment #2 92ml of sea water mixed with Cobalt chloride (400mg/1000ml concentration).

Experiment #3 92ml of sea water mixed with Cobalt chloride (1000mg/1000ml concentration).

Experiment #4 92ml of sea water mixed with Cobalt chloride (1000mg/1000ml concentration).

The experiments temperature Vs. time graph and is in **Figure A1**.

Table A9 summarizes the samples conditions and **Table A10** summarizes the monosaccharides released.

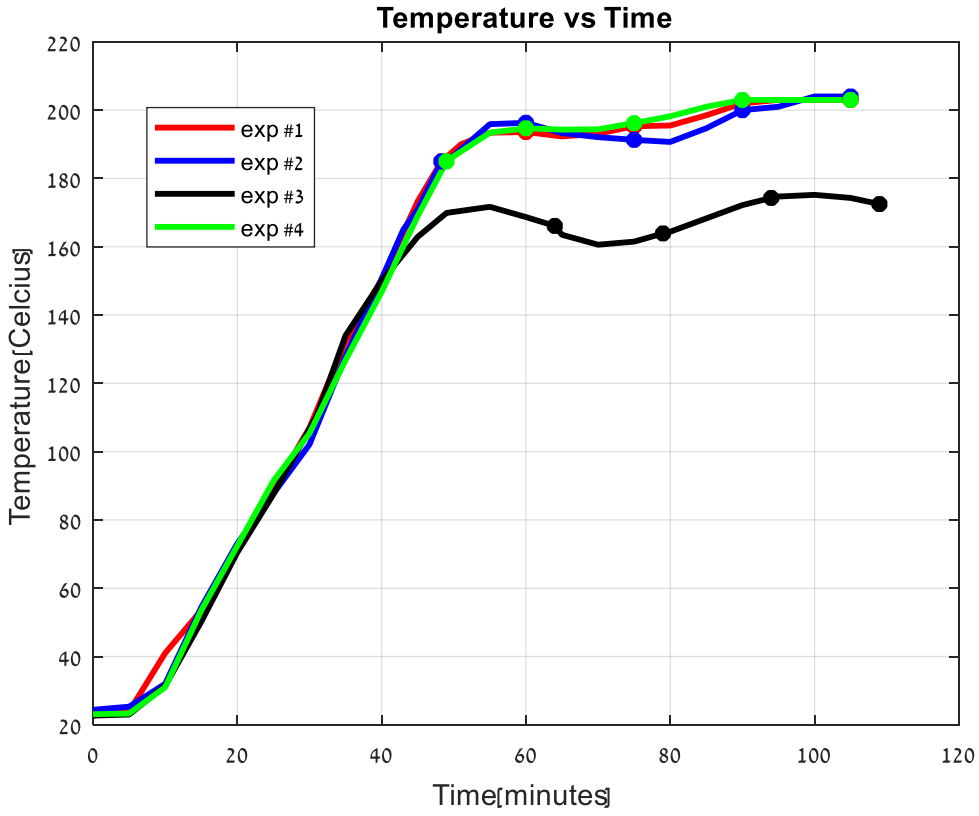

Figure A1- Cladophora experiments temperature vs time

Table A11. Sampling conditions (time and temperature)

	Exp. #1		Exp. #2		Exp. #3		Exp. #4	
Sample#	Time* (min)	Temp (^{0}C)	Time* (min)	Temp (^{0}C)	Time* (min)	Temp (^{0}C)	Time* (min)	Temp (^{0}C)
1	48.3	185	48.3	185	64	166.1	49	185
2	60	193.6	60	196.3	79	163.9	60	194.7
3	75	195.3	75	191.3	94	174.3	75	196.2
4	90	202	90	200	109	172.5	90	201
5	105	203	105	204			105	203

*measured from the beginning of the experiment.

Table A11. Cladophora released monosaccharaides

	Sample #	Arabinose mg/g	Galactose mg/g	Glucose mg/g	Xylose mg/g	Fructose mg/g	Total mg/g
Exp #1	1	0	0.02	1.71	4.1	4.19	9.95
	2	1.05	1.87	11.29	5.68	10.97	30.87
	3	3.85	4.32	22.62	3.93	5.55	40.28
	4	2.08	4.08	25.96	1.54	3.74	37.42
	5	1.21	3.51	24.76	1.22	3.75	34.46
Exp #2	1	0	0.12	0.71	0.14	0.06	1
	2	0.56	0.63	4.34	0.62	1.91	8
	3	5.35	5.22	30.43	2.63	2.4	46
	4	1.37	2	13.2	0.56	0.8	18
	5	0.2	0.91	5.12	0.13	0.43	6.8
Exp #3	1	0	0.22	0.74	0.76	0.63	2.34
	2	0.68	2.22	6.18	3	4.32	16.4
	3	1.3	3.89	11.8	5.16	7.44	29.6
	4	1.8	3.8	12	4.83	6.28	28.7
Exp #4	1	0	0	6.7	5.72	12.55	24.97
	2	0.67	1.97	10.95	5	12.2	30.9
	3	3.63	4.95	27.9	4.17	8.8	49.47
	4	1.75	4.2	28.62	1.65	5.58	41.8
	5	0.43	1.32	9.07	0.61	1.8	13.2

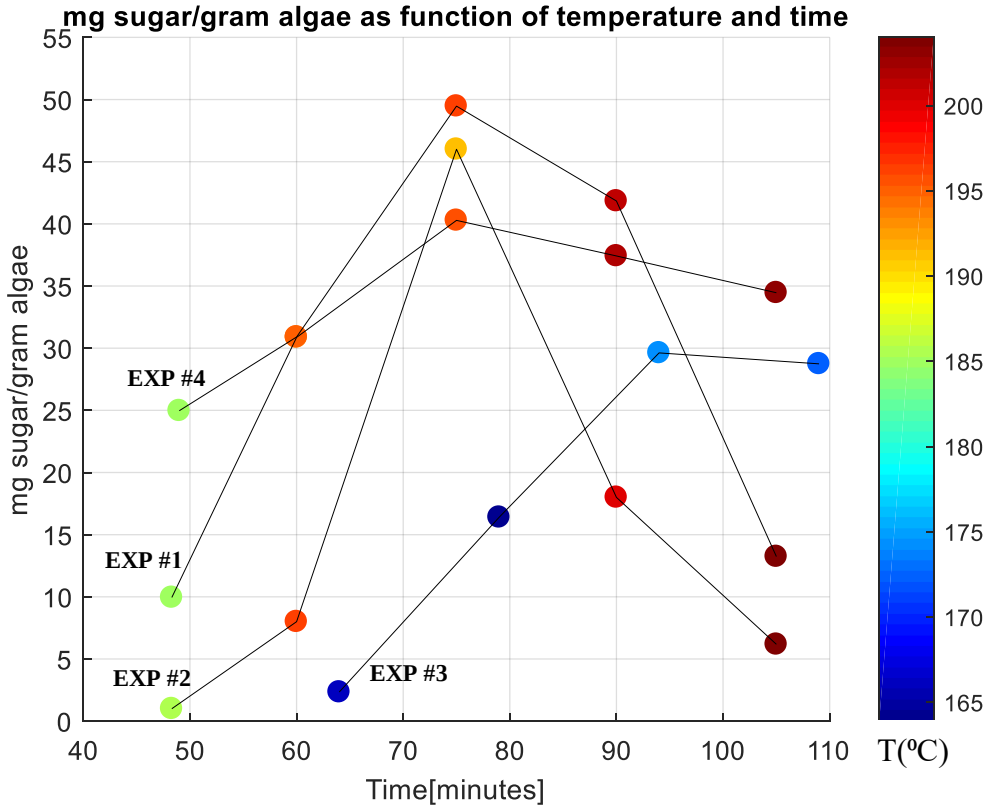

Figure A2- Cladophora experiments sugar yield

In the 3 higher temperature experiments (1,2,4) the maximum sugar yield is obtained at the same time with maximum yield increasing with catalyst concentration. The maximum sugar yield with catalyst is 49.47 mg/g and 40.28 mg/g without catalyst, 4 times higher than the *Ulva* sugar yield obtained in the Taguchi experiments. This could be partially due to the higher starch concentration in the *Cladophora* with 17.7% compared to 5.5% in the *Ulva*.

תקציר

פירוק ביומסה לסוכרים אשר יכולים לעבור התססה הינו אתגר גדול עבור בתי זיקוק ביולוגיים. שיטות מסורתיות עושות שימוש בחומצות אשר מזיקות לסביבה או בהידרוליזה אנזימטית אשר יקרה. הידרוליזה תרמית היא טכנולוגיה ירוקה עבור פירוק, ניזול וגזיפיקציה של ביומסה. עם זאת, הידרוליזה תרמית בתנאים תת קריטיים מייצרת מגוון רחב של תוצרים מחומר גלם הטרוגני כגון ביומסה. בעבודה זו, שיטת מערכים אורתוגונליים של טגוצ'י שימשו לתכנון הניסויים ולחקירת ההשפעה של הפרמטרים הבאים: טמפרטורת המים , זמן הטיפול, כמות מוצק ומליחות המים על יצירת גלוקוז, רמנוז, קסילוז, פרוקטוז וגלקטוז ממאקרו-אצה ירוקה. חומר גלם מתעורר בתעשיית בתי הזיקוק הביולוגיים. נבדקה גם ההשפעה של הפרמטרים הנ"ל על ייצור של 5-hydroxymethylfurfural, כימיקל אשר ניתן לייצר ממנו דלק ביולוגי, אך גם ידוע כמעכב תסיסה. נמצא כי עבור כל שחרור הסוכרים, טמפרטורת הריאקציה הינה הפרמטר המשמעותי ביותר, אחריו מליחות המים, כמות המוצק ולבסוף זמן הטיפול. טמפרטורה היא גם הפרמטר החשוב ביותר לייצור (5-HMF), אחריו זמן הטיפול, מליחות המים ולבסוף כמות המוצק. נקבעו הפרמטרים עבור תהליך אופטימלי לשחרור מקסימלי של כל החד-סוכרים וייצור מינימלי של (5-HMF). כמו כן, ההרכב הכימי והערך הקלורי של המוצק שנשאר לאחר הטפול (הידרו-פחם) נמדדו. בעזרת הערכים שנמצאו בניסויים בוצעה סימולציה אשר משלבת ייצור חשמל מאנרגיה השמש וייצור דלק (אתנול) מהסוכרים .נמצא כי הנצילות של הפקת חשמל דומה לזו של מתקנים סולאריים מקובלים. כמו כן, התפוקה האנרגטית של האתנול זניחה לעומת התפוקה האנרגטית של ההידרו-פחם ולעומת ההספק הסולארי הדרוש לתהליך.

אוניברסיטת תל אביב

הפקולטה להנדסה על שם איבי ואלדר פלישמן

בית הספר לתארים מתקדמים על שם זנדמן-סליינר

פירוק סולארי-הידרותרמי של ביומסת מאקרו-אצה ירוקה להפקת ביו-דלקים

חיבור זה הוגש כעבודת גמר לקראת התואר "מוסמך אוניברסיטה" בהנדסת סביבה

על-ידי

סמיון גרייסרמן

העבודה נעשתה בתוכנית להנדסת סביבה

בהנחיית פרופ' אברהם קריבוס וד"ר אלכסנדר גולברג

תשרי תשע"ט

אוניברסיטת תל אביב

הפקולטה להנדסה על שם איבי ואלדר פלישמן

בית הספר לתארים מתקדמים על שם זנדמן-סליינר

פירוק סולארי-הידרותרמי של ביומסת מאקרו-אצה ירוקה להפקת ביו-דלקים

חיבור זה הוגש כעבודת גמר לקראת התואר "מוסמך אוניברסיטה" בהנדסת סביבה

על-ידי

סמיון גרייסרמן

תשרי תשע"ט